THE ASTROPHYSICAL JOURNAL, 549:55–71, 2001 March 1


# ABUNDANCES AND EVOLUTION OF LITHIUM IN THE GALACTIC HALO AND DISK[1]

SEAN G. RYAN
Department of Physics and Astronomy, The Open University, Walton Hall, Milton Keyes MK7 6AA, UK; s.g.ryan@open.ac.uk

TOSHITAKA KAJINO
National Astronomical Observatory of Japan, Osawa 2-21-1, Mitaka, Tokyo 181-8588, Japan; and Department of Astronomy, University of Tokyo, 7-3-1 Hongo, Bunkyo-ku, Tokyo 113-0015, Japan; kajino@ferio.mtk.nao.ac.jp

TIMOTHY C. BEERS
Department of Physics and Astronomy, Michigan State University, East Lansing, MI 48824; beers@pa.msu.edu

TAKERU KEN SUZUKI
National Astronomical Observatory of Japan, Osawa 2-21-1, Mitaka, Tokyo 181-8588, Japan; and Department of Astronomy, University of Tokyo, 7-3-1 Hongo, Bunkyo-ku, Tokyo 113-0015, Japan; stakeru@th.nao.ac.jp

DONATELLA ROMANO
Scuola Internazionale Superiore di Studi Avanzati, International School for Advanced Studies, via Beirut, 2-4, 34014, Trieste, Italy; romano@sissa.it

FRANCESCA MATTEUCCI
Dipartimento di Astronomia, Università di Trieste, via G. B. Tiepolo 11, 34131 Trieste, Italy; and Scuola Internazionale Superiore di Studi Avanzati, International School for Advanced Studies, via Beirut, 2-4, 34014, Trieste, Italy; matteucci@ts.astro.it

AND

KATARINA ROSOLANKOVA
Department of Physics and Astronomy, The Open University, Walton Hall, Milton Keyes MK7 6AA, UK; katarina.rosolankova@st-hildas.oxford.ac.uk
*Received 2000 April 11; accepted 2000 October 17*

## ABSTRACT

We have measured the Li abundance of 18 stars with $-2 \lesssim$ [Fe/H] $\lesssim -1$ and $6000 \lesssim T_{\rm eff} \lesssim 6400$ K, a parameter range that was poorly represented in previous studies. We examine the Galactic chemical evolution (GCE) of this element, combining these data with previous samples of turnoff stars over the full range of halo metallicities. We find that $A$(Li) increases from a level of $\sim$2.10 at [Fe/H] $= -3.5$ to $\sim$2.40 at [Fe/H] $= -1.0$, where $A(\mathrm{Li}) = \log_{10}(n(\mathrm{Li})/n(\mathrm{H})) + 12.00$. We compare the observations with several GCE calculations, including existing one-zone models and a new model developed in the framework of inhomogeneous evolution of the Galactic halo. We show that Li evolved at a constant rate relative to iron throughout the halo and old disk epochs but that during the formation of young disk stars, the production of Li relative to iron increased significantly. These observations can be understood in the context of models in which postprimordial Li evolution during the halo and old disk epochs is dominated by Galactic cosmic-ray fusion and spallation reactions, with some contribution from the $\nu$-process in supernovae. The onset of more efficient Li production (relative to iron) in the young disk coincides with the appearance of Li from novae and asymptotic giant branch (AGB) stars. The major challenge facing the models is to reconcile the mild evolution of Li during the halo and old disk phases with the more efficient production (relative to iron) at [Fe/H] $> -0.5$. We speculate that cool-bottom processing (production) of Li in low-mass stars may provide an important late-appearing source of Li, without attendant Fe production, that might explain the Li production in the young disk.

*Subject headings:* cosmology: observations — early universe — Galaxy: halo — nuclear reactions, nucleosynthesis, abundances — stars: abundances — stars: Population II

## 1. INTRODUCTION

Lithium plays several valuable roles as a diagnostic of stellar and Galactic evolution. As the only metal synthesized in significant quantities in the big bang, $^7$Li provides a rare constraint on the baryon density of the universe (e.g., Ryan et al. 2000). As an element destroyed in stars where the temperature exceeds $2.5 \times 10^6$ K, its survival at the stellar surface indicates the degree of exchange of material between the surface and interior via convection, diffusion, and other processes. Thirdly, as a product of spallation and fusion reactions and of stellar sources, it provides a measure of the chemical evolution of the Galaxy.

In practice, the three roles of Li cannot be treated in isolation. The primordial (big bang) abundance cannot be determined without knowing the sources and sinks of the element, and the degree of mixing for stars of different metallicity cannot be determined from the observations unless the contribution of Galactic production is known. Normally, one attempts to reduce the complexity of the problem by isolating one or two parts. For example, the near constancy of the $^7$Li abundance in warm halo stars over a range of effective temperature and metallicity led Spite & Spite (1982) to conclude that destruction of Li in those stars and its production in the course of Galactic chemical evolution were negligible. As a result, they argued that it was proper to consider the observed Li abundance as the primordial one, hardly altered. The view that Li in these objects was unaltered was supported empirically by the small spread in Li abundances and by classical stellar evolu-

[1] Based on observations obtained with the University College London échelle spectrograph (UCLES) on the Anglo-Australian Telescope (AAT) and the Utrecht échelle spectrograph (UES) on the William Herschel Telescope (WHT).

tion models (e.g., Yale "standard" models; Deliyannis, Demarque, & Kawaler 1990), which showed negligible levels of pre–main-sequence and main-sequence destruction even over the long ($\simeq$13 Gyr) lives of the objects. (This contrasted with the considerable destruction seen in some young open clusters [e.g., Hobbs & Pilachowski 1988] but is understood as the depth of the surface convection zone being less in stars of lower metallicity, thus not reaching the depths required for burning at $T \geq 2.5 \times 10^6$ K.)

Challenges to the Li survival hypothesis have come from both theoretical and observational sources. More complex (and hopefully more realistic, but also more uncertain) stellar evolution models, involving rotationally induced mixing, were found to be able to deplete significant fractions of the Li in these objects. Early models suggested as much as 90% could be lost (Pinsonneault, Deliyannis, & Demarque 1992), though later work suggested that perhaps half might be destroyed (Pinsonneault et al. 1999). (The downward revision of the figure was driven partly by the models and partly by observational data.) Coupled to this theoretical work were claims of significant scatter in the observed abundances, inconsistent with a single primordial value (Deliyannis, Pinsonneault, & Duncan 1993; Thorburn 1994). The most recent observations show, however, that the intrinsic scatter in a sample of 22 halo field turnoff stars is $\sigma_{\rm int} < 0.02$ dex and does not support the proposition of more than 0.1 dex $^7$Li depletion by the rotational mixing mechanism (Ryan, Norris, & Beers 1999). Although this field star sample places very tight limits on the intrinsic spread in $^7$Li, there is evidence of at least some star-to-star differences in the halo. Boesgaard et al. (1998) find a spread in $^7$Li abundance among subgiants in M92 (see Fig. 1), while C. P. Deliyannis (1999, private communication) finds $^7$Li differences between the extremely metal-poor field stars G64-12 and G64-37, stars that otherwise appear very similar to one another. Furthermore, there exist a small number of very Li-deficient stars that are otherwise indistinguishable from halo Li "preservers" (Hobbs, Welty, & Thorburn 1991; Thorburn 1992; Spite et al. 1993; Norris et al. 1997; Ryan, Norris, & Beers 1998). However, the different (dense) stellar environment of the M92 stars and small volume of the Galaxy it samples, as well as the rarity of the other cases, lead us to view the small observed spread of Li abundance in the recent halo star sample ($\sigma_{\rm int} < 0.02$) as representative of the majority of the halo.

In addition to discussions of the intrinsically thin Spite halo Li plateau, claims have been made of the existence of dependencies of observed Li abundance upon $T_{\rm eff}$ and [Fe/H]. Thorburn (1994), Norris, Ryan, & Stringfellow (1994), and Ryan et al. (1996a) all found the halo observations to require significantly nonzero coefficients to fits of the form $A({\rm Li}) = A_0 + A_1(T_{\rm eff}/100\ {\rm K}) + A_2[{\rm Fe/H}]$, where $A({\rm Li}) = \log_{10}(n({\rm Li})/n({\rm H})) + 12.00$. Typical estimated values of the coefficients were $A_1 = 0.03$ and $A_2 = 0.14$. The coefficient on $T_{\rm eff}$, $A_1$, may depend crucially on the adopted temperature scale. The optical photometric scales used in the cited studies were challenged by Bonifacio & Molaro (1997), who used temperatures derived from application of the infrared flux method (IRFM), whereupon they concluded that both $A_1$ and $A_2$ were consistent with zero, which is to say that the Spite plateau is flat. The IRFM scale has often been proposed as less likely to be affected by metallicity-dependent systematic errors (Saxner & Hammarbäck 1985; Magain 1987), but the uncertainties in the $T_{\rm eff}$ of any individual star are still considerable, with $\sigma_{T_{\rm eff}} \simeq 100$ K (Alonso, Arribas, & Martínez-Roger 1996; Bonifacio & Molaro 1997). The other photometric scales can at least lead to small internal errors, $\sigma_{T_{\rm eff}} \simeq 30$–40 K (Ryan et al. 1999), and a mean error of 55 K in the present sample, but possibly with less reliable external systematics. The tradeoff is that the IRFM may deliver better systematics but at the expense of introducing greater internal scatter. Hopefully, improvements in the systematics of the optical temperature scales and in the internal errors of the IRFM scale will be achieved, and we will be able to clarify the size of the $A_1$ term in the near future.

Bonifacio & Molaro (1997) also found the $A_2$ term (metallicity coefficient) to be consistent with zero, but the work by Ryan et al. (1999), which achieved errors as small as $A({\rm Li}) = 0.03$ dex for most stars, again found a significant value: $A_2 = 0.118 \pm 0.023$. Ryan et al. (1999) traced the main difference between these two results to some substantial differences in the stellar metallicities adopted (from the literature) by the two studies. After comparing with a third [Fe/H] estimate (the homogeneously applied estimator of metallicity obtained by Beers et al. 1999), they argued that the [Fe/H] values adopted by Bonifacio & Molaro (1997) had sufficiently large errors to obscure the $A_2$ analysis. Ryan et al. (1999) further argued that measurements of $^6$Li in HD 84937 and BD +26°2578 (Smith, Lambert, & Nissen 1993, 1998; Cayrel et al. 1999; Hobbs & Thorburn 1994, 1997), and now also in HD 140283 (C. P. Deliyannis & S. G. Ryan 2001, in preparation), likewise evidenced the contribution of Galactic chemical evolution (GCE) to Li production even in stars with [Fe/H] $\sim -2.5$, since $^6$Li is thought to be exclusively postprimordial. The contributions to the total Li inferred from $A_2$ and from $^6$Li were found to be compatible. From application of the inhomogeneous GCE model of Suzuki, Yoshii, & Kajino (1999), Suzuki, Yoshii, & Beers (2000) argue that a nonzero slope in the relationship between $A$(Li) and [Fe/H] (of the same order of magnitude as that observed) must arise in the early Galaxy from Li production associated with the spallation reactions that give rise to Be and B.

In their earlier study, Ryan et al. (1996a) noted that an observational bias existed in the available Li data for halo stars. In the quest for the primordial lithium abundance, observers had studied progressively more metal-poor stars but had examined rather fewer at [Fe/H] $\sim -1.5$. Moreover, those that were examined at higher [Fe/H] were invariably cooler than the more metal-poor ones, potentially complicating the analysis of the coefficients $A_0$, $A_1$,

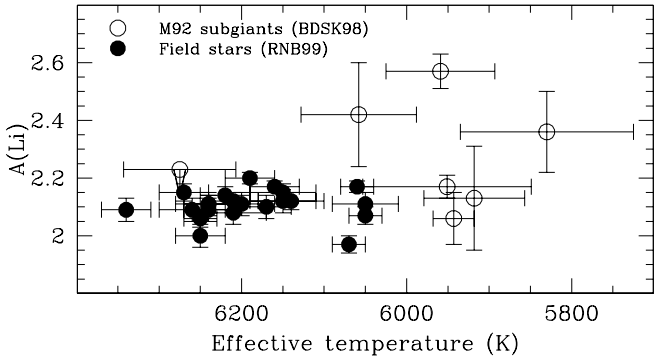


FIG. 1.—Li spread in halo field and globular cluster samples

and $A_2$ by the inadvertent introduction of collinearity in the predictor variables. To address both of these difficulties, we set out to measure a sample of hotter ($6000 \lesssim T_{\rm eff} \lesssim 6400$ K), more metal-rich ($-2 \lesssim$ [Fe/H] $\lesssim -1$) stars. The sample selection, observations, and abundance analysis are discussed in the following sections. We then combine the new data on 14 stars, which correct the previous paucity of warmer, higher metallicity halo stars with existing observations, and examine the GCE of Li. In addition to these 14 stars, we report on four stars with $A$(Li) < 1.7, two of which are newly discovered extremely Li-deficient halo stars. These exceptional stars are discussed in detail in a separate paper (Ryan et al. 2001).

## 2. SAMPLE SELECTION, OBSERVATIONS, AND ABUNDANCE ANALYSIS

### 2.1. *Sample Selection and Observation*

We sought to address two problems: (1) the lack of Li measurements in stars with $-2 \lesssim$ [Fe/H] $\lesssim -1$, with which to study the GCE of this element; and (2) the selection bias against warm stars with $6000 \lesssim T_{\rm eff} \lesssim 6400$ K in this metallicity interval. We searched the catalogs of Schuster & Nissen (1988, 1989), Schuster, Parrao, & Contreras Martinez (1993), Ryan (1989), Ryan & Norris (1991), and Carney et al. (1994) for stars in these [Fe/H] and $T_{\rm eff}$ ranges. Observations were obtained with the University College London échelle spectrograph (UCLES) on the Anglo-Australian Telescope (AAT) on 1996 September 24 and with the Utrecht échelle spectrograph (UES) on the William Herschel Telescope (WHT) on 1997 August 23. Both spectrographs, which have almost identical configurations, were set up to deliver $\lambda/\Delta\lambda \simeq 50{,}000$ at the Li 6707 Å doublet. Both observing runs utilized 79 line mm$^{-1}$ gratings, which allow a slit length of 14″ to ensure adequate sampling of the background (sky and scattered light) contribution.

The stars for which spectra were obtained are listed in Table 1. Column (1) lists the star name(s). Columns (2) and (3) list the 2000.0 epoch positions. Apparent magnitudes and colors, as well as estimates of the reddening in the direction to each star, taken from the references listed above, are listed in columns (4)–(9).[2] The [Fe/H] measurements provided in column (10), also taken from the references above, are based on either medium-resolution spectra or photometric estimates that, over this metallicity range, are expected to be accurate to $\sigma_{\rm [Fe/H]} = 0.15$–$0.20$ dex (Schuster & Nissen 1989; Ryan & Norris 1991; Carney et al. 1994). Five of the stars in Table 1 have independent estimates of [Fe/H] derived from medium-resolution spectroscopy reported by Beers et al. (1999). The mean offset is $[{\rm Fe/H}]_{\rm AK2} - [{\rm Fe/H}]_{\rm lit} = -0.08$, with an rms scatter of 0.13 dex, which provides additional evidence that the metallicities used herein are secure.

Errors in [Fe/H] will affect the Li abundances derived below in three ways. First, they will cause a model atmosphere of the wrong metallicity to be used. The impact of this is completely negligible, as Table 5 of Ryan et al. (1996a) shows. A star with $T_{\rm eff} = 6300$ K, [Fe/H] $\simeq -1.5$, and $A$(Li) = 2.20 would give rise to an error in $A$(Li) of only 0.002 dex for a 0.2 dex error in [Fe/H]. Secondly, an error in [Fe/H] would also cause an incorrect effective temperature to be adopted. In the $b-y$ calibrations of Magain (1987), a metallicity error of 0.2 dex at [Fe/H] = $-1$ and $T_{\rm eff} = 6300$ K would induce a temperature error of 12 K, which corresponds to only 0.010 dex in $A$(Li). This error must of course be added to those arising from the other sources. Thirdly, an error in [Fe/H] would cause a star to be shifted along the $x$-axis in an $A$(Li)-versus-[Fe/H] diagram; the impact of the error in that case depends on the model to which the data are being compared and can be assessed from the error bars shown in such a figure.

### 2.2. *Effective Temperatures and Uncertainties*

Effective temperatures were calculated using the same $B-V$, $R-I_{\rm C}$, and $b-y$ calibrations as in Ryan et al. (1996a) to maintain consistency with that work, but with the addition of the $V-R_{\rm C}$ calibration of Bell & Oke (1986). Ryan et al. (1996a) found "very good agreement between $B-V$ and $b-y$ temperatures" but reported that "the $R-I$ temperatures exceed the $B-V$ temperatures on average by perhaps 50 K for the cooler half of the sample, but the systematics are too marginal to justify adjusting the scales further." As we will combine our present sample with that of Ryan et al. (1996a), to assess the impact of including hotter, more metal-rich stars, we utilize the same procedure.

In contrast to the result for the broad 1996 sample where systematic differences were "too marginal to justify adjusting the scales," Ryan et al. (1999) found some well-defined and larger offsets for the Bell & Oke (1986) scales in a narrowly defined subset of very metal-poor ([Fe/H] $\lesssim$ -2.2) and hotter ($T_{\rm eff} \gtrsim 6000$ K) stars. For this narrowly defined subset of stars, offsets were made to the Bell & Oke (1986) scales for those very metal-poor stars of up to 165 K. Because such offsets were not discernible for the broad (1996) sample, one may be concerned about the impact of unadjusted systematic errors that remain embedded in the Ryan et al. (1996a) temperatures. For this reason, we adopted a more conservative approach in this work compared with Ryan et al. (1996a) for computing the *uncertainties* on $T_{\rm eff}$.

To recap, Ryan et al. (1996a) propagated errors in each individual photometric index and the reddening estimates and combined these on the assumption that they fully captured the error sources. A more conservative approach would have been to take the greater of this value or the index-to-index standard deviation where two or more colors were available. Indeed, we adopt this more conservative approach in the current work. As we inspect the index-to-index scatter, our revised approach will also be inflated by any imbedded systematic differences between different temperature scales used in the $T_{\rm eff}$ calculation. However, we find that the more conservative approach makes very little difference quantitatively. The uncertainties for the current work ranged up to 130 K, with a mean value of 55 K. To be especially conservative, we assigned this mean estimate to stars with only a single color and to those stars whose formal estimate was (probably fortuitously) less than 55 K. That is, an error in $T_{\rm eff}$ of 55 K is the *smallest* we claim in the current work. In comparison, the errors reported in the 1996 study ranged from 32 to 180 K, with a mean of 52 K. The resulting difference between approaches has almost no effect on the claimed mean error or even the range of errors deduced. Had we considered the index-to-index scatter in

[2] Although no preselection on Li abundance was made in the assemblage of our sample, one unexpected result was the inclusion of four Li-deficient stars, two of which were new discoveries. Table 1 is therefore separated into two parts in recognition of this.

TABLE 1

PROGRAM STARS AND LI MEASUREMENTS

| Star (1) | R.A. (2000) (2) | Decl. (2000) (3) | $V$ (4) | $B-V$ (5) | $V-R$ (6) | $R-I$ (7) | $b-y$ (8) | $E(B-V)$ (9) | [Fe/H] (10) | $T_{\rm eff}$ (K) (11) | $\sigma_T$ (K) (12) | Tel.[a] (13) | S/N (14) | $W$ (mÅ) (15) | $\sigma_W$ (mÅ) (16) | $A$(Li) (17) | $\sigma_{A(\rm Li)}$ (18) |
|---|---|---|---|---|---|---|---|---|---|---|---|---|---|---|---|---|---|
| **Spite Plateau Stars** | | | | | | | | | | | | | | | | | |
| HD 16031[b] (BD −13°482)..... | 023411.05 | −122303.5 | 9.77 | 0.45 | ... | ... | 0.324 | 0.01 | −1.83 | 6038 | 90 | A | 70 | 25.7 | 2.6 | 2.09 | 0.07 |
| BD +19°1730 (G88-27)..... | 072702.34 | 190555.4 | 10.73 | 0.44 | 0.30 | 0.30 | 0.336 | 0.02 | −1.47 | 6058 | 100 | W | 68 | 35.8 | 2.7 | 2.27 | 0.07 |
| BD +17°4708 (G126-62)..... | 221131.37 | 180534.1 | 9.48 | 0.44 | 0.30 | 0.32 | 0.33 | 0.01 | −1.86 | 5983 | 69 | W | 86 | 29.2 | 2.2 | 2.11 | 0.05 |
| BD +00°2058A (G112-43)..... | 074343.97 | −000400.9 | 10.22 | 0.45 | ... | ... | 0.34 | 0.02 | −1.48 | 6034 | 55 | A | 56 | 37.6 | 3.3 | 2.28 | 0.05 |
| BD −03°5166..... | 211719.07 | −024452.7 | 10.84 | 0.45 | 0.30 | 0.31 | ... | 0.04 | −1.33 | 6178 | 82 | W | 73 | 31.1 | 2.5 | 2.29 | 0.06 |
| CD −30°18140 ..... | 204406.29 | −300007.5 | 9.95 | 0.41 | 0.28 | 0.31 | 0.323 | 0.04 | −2.10 | 6270 | 55 | W | 59 | 32.4 | 3.1 | 2.37 | 0.05 |
| CD −30°18140 ..... | 204406.29 | −300007.5 | 9.95 | 0.41 | 0.28 | 0.31 | 0.323 | 0.04 | −2.10 | 6270 | 55 | A | 70 | 28.8 | 2.6 | 2.32 | 0.05 |
| CD −31°305 (G267-178) ..... | 005013 | −303606 | 11.67 | 0.44 | 0.30 | 0.31 | ... | 0.00 | −1.02 | 5967 | 130 | W | 81 | 38.6 | 2.2 | 2.24 | 0.09 |
| CD −33°239 (G267-150) ..... | 003951 | −330312 | 11.00 | 0.43 | 0.28 | 0.31 | ... | 0.00 | −1.87 | 5993 | 55 | A | 92 | 28.9 | 2.0 | 2.11 | 0.05 |
| G75-31 ..... | 023821.51 | 022644.4 | 10.50 | 0.465 | 0.30 | 0.32 | 0.333 | 0.01 | −1.15 | 5981 | 66 | W | 89 | 48.0 | 2.1 | 2.36 | 0.05 |
| G87-13 ..... | 065456 | 353112 | 11.06 | 0.48 | ... | ... | 0.346 | 0.04 | −1.23 | 6077 | 55 | W | 64 | 46.4 | 2.9 | 2.42 | 0.04 |
| G126-10..... | 213500.22 | 105514.3 | 11.83 | 0.465 | ... | ... | 0.35 | 0.04 | −1.37 | 6086 | 55 | W | 84 | 34.2 | 2.2 | 2.27 | 0.04 |
| G192-43..... | 064744.94 | 583834.5 | 10.31 | 0.43 | ... | ... | 0.322 | 0.01 | −1.43 | 6130 | 55 | W | 77 | 34.5 | 2.4 | 2.31 | 0.05 |
| G245-32..... | 014712.39 | 732827.2 | 9.92 | 0.42 | ... | ... | ... | 0.04 | −1.62 | 6290 | 55 | W | 70 | 27.0 | 2.6 | 2.30 | 0.05 |
| LP 824-188 (G266-60) ..... | 001117 | −204324 | 11.82 | 0.45 | 0.29 | 0.33 | ... | 0.00 | −1.84 | 5890 | 75 | A | 53 | 30.8 | 3.5 | 2.07 | 0.07 |
| **Li-deficient Stars** | | | | | | | | | | | | | | | | | |
| −31°19466 (G275-111)..... | 235012 | −303418 | 11.41 | 0.44 | 0.29 | 0.30 | ... | 0.00 | −1.89 | 5986 | 78 | A | 65 | <7.5 | 2.8 | <1.49 | 0.05[c] |
| BD +51°1817 (G177-23)..... | 130839.10 | 510359.3 | 10.23 | 0.38 | ... | ... | ... | 0.00 | −1.10 | 6345 | 55 | W | 83 | <5.7 | 2.1 | <1.64 | 0.04[c] |
| G202-65..... | 163558.58 | 455159.3 | 11.22 | 0.36 | ... | ... | ... | 0.00 | −1.50 | 6390 | 55 | W | 82 | <6.0 | 2.2 | <1.67 | 0.04[c] |
| Wolf 550 (G66-30) ..... | 145007.81 | 005027.2 | 11.03 | 0.40 | 0.27 | 0.29 | 0.305 | 0.03 | −1.66 | 6269 | 55 | W | 78 | <6.3 | 2.4 | <1.61 | 0.04[c] |

[a] A = AAT; W = WHT.

[b] HD 16031 = LP 710-89.

[c] For stars with no Li detections, $W$ and $A$(Li) are based on the $3\sigma_W$ limit. The quoted uncertainties $\sigma_{A(\rm Li)}$ for their abundances reflect the $\sigma_T$ uncertainty.

1996, the mean error would have been only marginally increased, to 62 K.

As we will combine the present sample and the 1996 one, how should we regard the 1996 error estimates in hindsight? While a more conservative error estimation procedure could have been adopted, and some individual stars would certainly have had different values quoted, it appears that both the mean error and the range of errors quoted would not have been significantly different. Note also that these more conservative estimates are sensitive to embedded systematic differences between $T_{\rm eff}$ scales for different photometric indices, since these would increase the star-to-star scatter, yet the conservatively computed errors for the sample are similar in both range and mean. For this reason, we have chosen to adopt the published 1996 values unchanged.

As a final comment, we reemphasize that the discussion of errors here has centered on relative (star-to-star) differences. It is clear from the various color–versus–effective temperature transformations discussed that the adopted zero point could still be in error by 100 K or more. However, zero-point errors will affect most stars similarly and hence will result in an overall translation of observation data more so than a rearrangement of the data relative to one another.

### 2.3. *Spectral Analysis*

The spectra were reduced in IRAF using conventional techniques, and final data are shown in Figure 2. Table 1 records the telescope used and the S/N per 50 mÅ pixel (taken as the lesser of the S/N based on photon statistics and the measured scatter in the continuum) in columns (13) and (14), respectively. Equivalent widths of the Li lines, $W$, were measured for the stars in each of two ways. First, a Gaussian fit was made to the Li lines, and the equivalent width and FWHM were recorded. Once all stars were measured, the mean FWHM of the fitted Gaussians was computed for each spectrograph. A second series of measurements was then made, with the Gaussian FWHM for each spectrograph fixed at the mean value. This is done because the $^7$Li doublet, being broader than the instrumental resolution, is not expected to vary in FWHM from star to star since all have "weak" ($W/\lambda < 10^{-6}$) Li lines. Finally, the two equivalent width measurements were averaged and are listed in column (15) of Table 1. The error in the measured Li equivalent width, reported in column (16), is based on the error model $\sigma_W = 184/(\mathrm{S/N}_{50})$ (Ryan et al. 1999).

To maintain consistency with the analysis of Ryan et al. (1996a, 1999), the same computations of $A$(Li) from $T_{\rm eff}$, $W$, and [Fe/H] were used. To recap, these utilized R. A. Bell (1983, private communication) stellar atmosphere models and the spectrum synthesis code of Cottrell & Norris (1978) to compute the $^7$Li doublet using four components for the fine structure and hyperfine structure. The inferred abundances and their errors, given as the quadratic sum of separate terms for $\sigma_W$ and $\sigma_T$, are listed in the final columns of Table 1.

Figure 3 shows the distribution of the stars in our present analysis in the $T_{\rm eff}$-[Fe/H] plane. The new observations are seen to correct substantially the previous deficit of warmer, more metal-rich systems, though additional observations of similar stars are certainly warranted.

Radial velocities measured from our spectra are given in Table 2 (in km s$^{-1}$). The *internal* error estimates ($\sigma_v$, tabulated) are only 0.1–0.3 km s$^{-1}$, but similar work by us in the past has suggested an *external* error of 0.3 km s$^{-1}$ (Ryan et al. 1999). Previous measurements from échelle observations by Carney et al. (1994), which are accurate to $\sim$0.1 km s$^{-1}$, or from medium-resolution spectra of Ryan & Norris (1991), accurate to only $\sigma_v = 7$ km s$^{-1}$, are included for comparison. Stars already identified as spectroscopic binaries are explicitly noted. The mean difference $\langle v_{\rm rad} - v_{\rm CLLA94} \rangle = -0.35$ km s$^{-1}$, with an rms difference of 0.68 km s$^{-1}$. This is larger than the 0.3 km s$^{-1}$ accuracy expected and may indicate the presence of unidentified low-amplitude and/or long-period binaries in the sample.

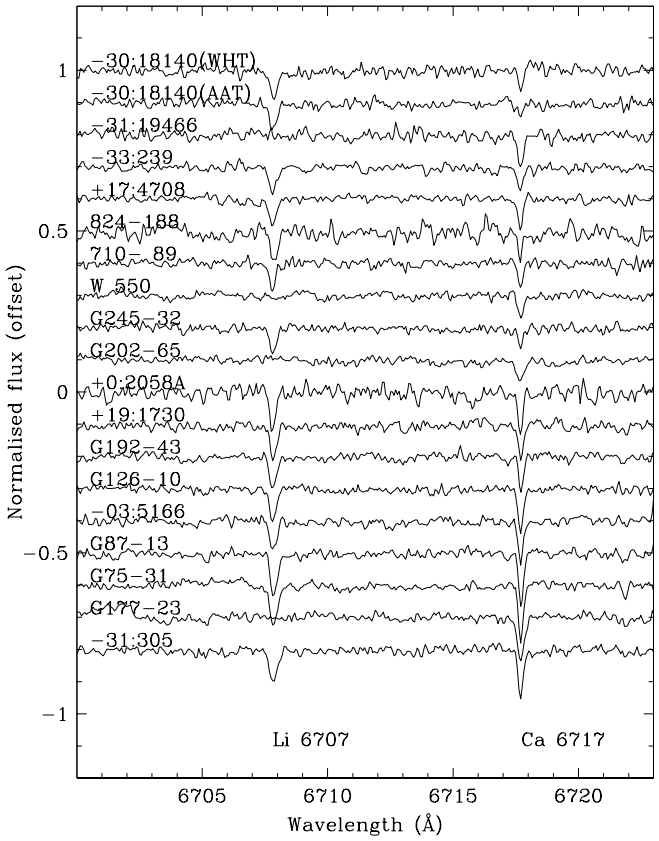


FIG. 2.—Spectra in the region of the Li 6707 doublet, in order of increasing [Fe/H]. Note the presence of four stars with greatly depressed Li abundances.

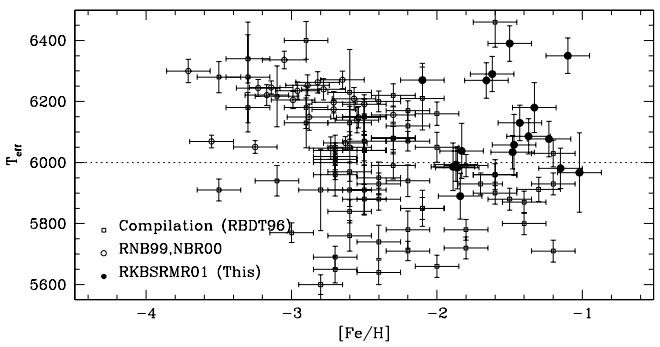


FIG. 3.—Location of program stars in the $T_{\rm eff}$-vs.-[Fe/H] plane, where they fill a deficit caused by selection biases in the literature. *Dotted line:* dividing line in sample at $T_{\rm eff} = 6000$ K.

TABLE 2

ABSOLUTE MAGNITUDES AND KINEMATICS

| Star (1) | $M_V$ (2) | $v_{rad}$ (3) | $\sigma_v$[a] (4) | $v_{prev}$[b] (5) | $U$ (6) | $V$ (7) | $W$ (8) |
|---|---|---|---|---|---|---|---|
| Spite Plateau Stars | | | | | | | |
| HD 16031 ..... | $4.5^{+0.4}_{-0.5}$ | 24.3 | 0.2 | 24.0 | −26 | −74 | −38 |
| BD +19°1730..... | $4.7^{+0.7}_{-0.9}$ | 43.9 | 0.1 | 44.3 | 24 | −189 | −100 |
| BD +17°4708..... | $4.1^{+0.3}_{-0.4}$ | −287.6 | 0.1 | SO | 242 | −271 | 38 |
| BD +00°2058A..... | ... | −83.6 | 0.1 | −84.2 | −121 | −66 | −166 |
| BD −03°5166..... | ... | −128.7 | 0.1 | −122 | −95 | −231 | 54 |
| CD −30°18140 ..... | $4.3^{+0.4}_{-0.5}$ | 17.4[c] | 0.2 | 17 | −48 | −196 | −31 |
| CD −30°18140 ..... | $4.3^{+0.4}_{-0.5}$ | 18.3[d] | 0.3 | 17 | −48 | −196 | −31 |
| CD −31°305..... | ... | 61.9 | 0.2 | ... | −155 | −249 | −44 |
| CD −33°239..... | ... | 94.4 | 0.2 | 98 | 81 | −258 | −89 |
| G75-31..... | $4.6^{+0.6}_{-0.9}$ | 56.7 | 0.1 | 57.4 | 164 | −135 | 43 |
| G87-13..... | ... | 205.0 | 0.1 | 206.4 | 194 | −163 | 36 |
| G126-10 ..... | ... | −101.5 | 0.1 | −101.7 | −237 | −192 | 77 |
| G192-43 ..... | $3.3^{+0.8}_{-1.3}$ | 190.1 | 0.2 | 191.1 | 265 | −128 | 29 |
| G245-32 ..... | $4.0^{+0.4}_{-0.5}$ | −269.4 | 0.1 | −269.0 | −259 | −138 | −6 |
| LP 824-188..... | $5.8^{+1.4}_{-5.6}$ | −108.2 | 0.3 | −96 | 316 | −150 | 45 |
| Li-deficient Stars | | | | | | | |
| CD −31°19466 ..... | ... | −113.5 | 0.2 | −95 | 123 | −322 | 48 |
| BD +51°1817..... | $4.2^{+0.5}_{-0.6}$ | −57.6 | 0.1 | SO | −60 | −153 | 20 |
| G202-65 ..... | $3.0^{+1.1}_{-2.4}$ | −249.6 | 0.1 | SO | 253 | −195 | −47 |
| Wolf 550..... | $5.3^{+0.7}_{-0.9}$ | −122.3 | 0.2 | SO | 225 | −245 | 16 |

[a] $\sigma_v$ gives the formal internal error in $v_{rad}$. An external error of 0.3 km s$^{-1}$ probably should be added; see text.

[b] Previous radial velocity measurements given to one decimal place are from Carney et al. 1994. Data to zero decimal places are lower resolution measurements of Ryan & Norris 1991 for which $\sigma_v = 7$ km s$^{-1}$. The code "SO" is used for previously known spectroscopic binaries (Carney et al. 1994).

[c] WHT observation.

[d] AAT observation.

However, the largest absolute value residual against the Carney et al. (1994) measurements is only 1.4 km s$^{-1}$, making it difficult to distinguish the remaining binaries with certainty. Residuals between the new data and the measurements of Ryan & Norris (1991) are consistent with the velocity errors arising from the lower resolution of those older data.

Any concern whether the stars genuinely belong to the halo rather than the disk populations (since metallicity alone is a poor discriminant at intermediate abundances) can be dispelled by consideration of the $U$, $V$, and $W$ space velocities. Those shown in columns (6)–(8) of Table 2 are heliocentric velocities from Ryan & Norris (1991), or local standard of rest (LSR) velocities from Carney et al. (1994) if the former are not available. The sole exception is BD −31°305, which had not been studied in those works and was computed here following the precepts of Ryan & Norris (1991). The Ryan & Norris (1991) velocities are used in preference because their distance scale shows better agreement with *Hipparcos* measurements for the program stars (see Fig. 4); the Carney et al. (1994) distances tend to underestimate those from *Hipparcos*. All except HD 16031 have velocities in excess of 100 km s$^{-1}$, some substantially so, removing any doubt that they are correctly associated with the halo. For completeness, we also tabulate absolute $V$ magnitudes based on *Hipparcos* parallaxes (and errors) in column (2) of the table.

## 3. THE Li ABUNDANCES

Figure 5 shows the newly obtained Li abundances, along with the literature sample, for the abundance interval $-2.2 < [Fe/H] < -1.0$, representing an extension of the sample discussed by Ryan et al. (1996a) in their Figure 3*b*. (We restrict the sample to an $\sim$1 dex interval of [Fe/H] because any metallicity dependence would increase the spread in this diagram.) The new observations are consistent with the older data and show that the results of the 1996 analysis, as well as the claim of the existence of a significant dependence of $A$(Li) on $T_{eff}$, were not caused by the inherited selection bias against more metal-rich turnoff stars illustrated in Figure 3. We quantify this statement below.

Having added data to the high-metallicity regime, and also now having the benefit of the improved observations of Ryan et al. (1999), it is important to ask whether the correlations between $A$(Li), $T_{eff}$, and [Fe/H] found by Ryan et al. (1996a) are still present. As the current paper is primarily a study of GCE, we only present an abbreviated discussion of the correlations here and refer the reader interested in a more detailed statistical analysis to Appendix A.

We have performed bivariate fits of the form $A(\mathrm{Li}) = A_0 + A_1(T_{eff}/100) + A_2[\mathrm{Fe/H}]$ to the stellar sample (sample A, comprising 94 stars) assembled in Ryan et al. (1996a). Sample B is an update and extension of sample A to 109 stars, where we have included the new observations from this paper and the improved abundances of Ryan et al. (1999), Norris, Beers, & Ryan (2000), and Spite et al. (2000), who give an abundance for CS 29527-015 that previously had only an upper limit on its Li abundance. As in the previous work, three least-squares regression routines have

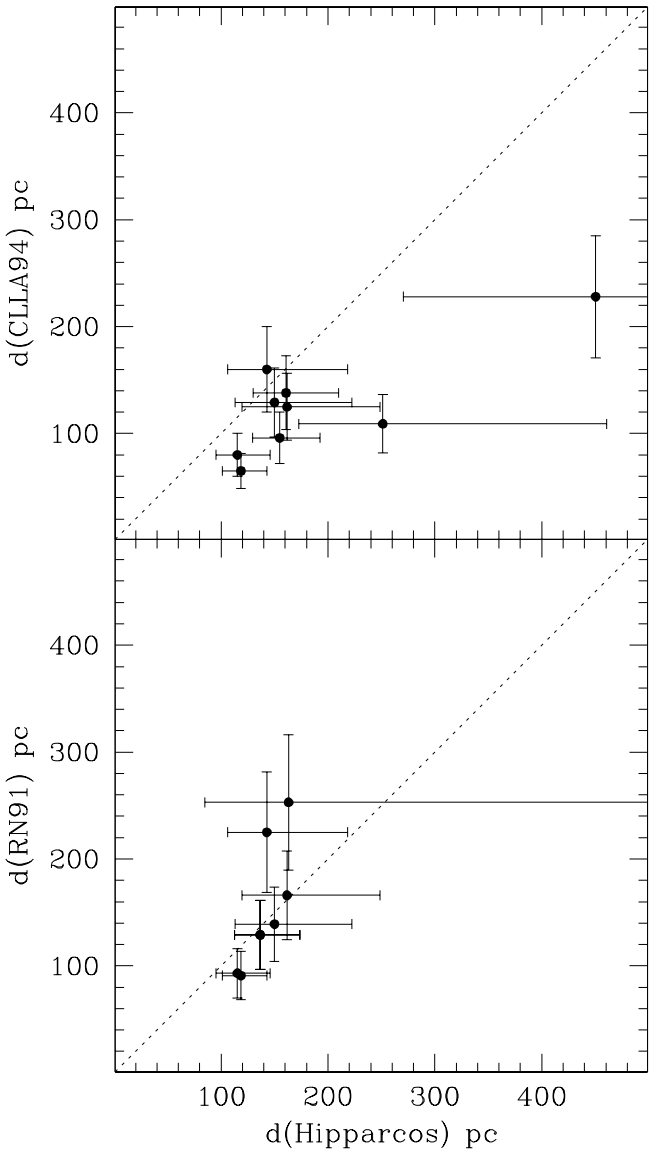


FIG. 4.—Comparison of photometric distance scales of Carney et al. (1994) and Ryan & Norris (1991) with *Hipparcos* data. Uncertainties in the photometric scales are taken as 25%, whereas the *Hipparcos* uncertainties are taken directly from the catalog.

been employed: a weighted least-squares (WLS) approach, an unweighted (standard) least-squares approach (LS), and a reweighted least-squares approach based on the least median of squares (RLS/LMS) algorithm with outlier rejection (see Ryan et al. 1996a and Appendix A of this paper for details).

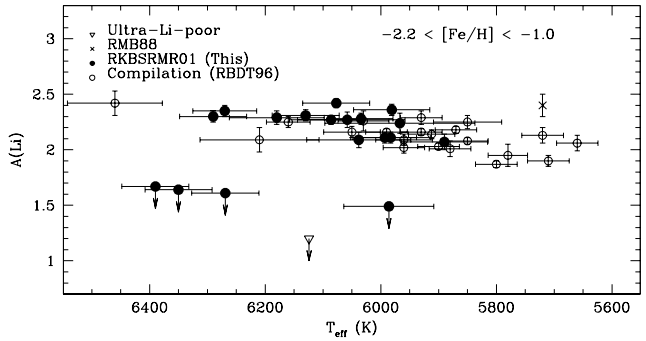


FIG. 5.—Variation of $A$(Li) with $T_{\rm eff}$ for stars with $-2.2 < [{\rm Fe/H}] < -1.0$. *Solid symbols*: new data; *open symbols*: previous data from literature. It is unclear whether the trend is real or caused by deficiencies in the color-temperature transformation, but the new data indicate that it is not due to selection biases in previous studies. Note also the four ultra–Li-depleted stars.

Table 3 provides the coefficients of the fits and their standard 1 $\sigma$ errors. The coefficient of determination, $R^2$, which is a measure of the amount of variance in $A$(Li) that can be accounted for by the regression model, is also given. The main conclusion to be drawn from Table 3, seen by comparing the sample A and sample B results, is that even though Ryan et al. (1996a) were working with biased and inferior data to those now available, the coefficients associated with $T_{\rm eff}$ and [Fe/H] are essentially unchanged from the earlier analysis. Addition of the hotter, more metal-rich stars has not weakened any of the earlier arguments; in fact, the coefficients of determination have all risen. Of course, in and of itself, this does not establish the *reality* of the $T_{\rm eff}$ trend, as we have intentionally used the same temperature scale as before; the scale could contain systematic errors as Bonifacio & Molaro (1997) suggest in their IRFM study. We hope that the reality, or otherwise, of the $T_{\rm eff}$ trend will be established reliably once the halo temperature scale is known with greater certainty. We note in closing this topic that the coefficients were not significantly affected by choosing a higher low-temperature limit (5800 K) for the sample.

In Figure 6 (*top panel*) we plot the available halo data in the $A$(Li)-versus-[Fe/H] plane. Observations of young and old disk stars by Boesgaard & Tripicco (1986), Rebolo, Molaro, & Beckman (1988), Lambert, Heath, & Edvardsson (1991), and Nissen et al. (1999) are included to show the evolution of Li beyond the halo phase. The present sample of halo stars with $[{\rm Fe/H}] > -2$ confirms that the metallicity dependence of $A$(Li) discussed above continues right up to the highest halo metallicities. However, as this figure contains a wide range of effective temperatures, and we are concerned about a nonzero dependence of $A$(Li) on that parameter (be it genuine or artificial), we restrict the sample shown in Figure 6 (*bottom panel*) to include only the hottest

TABLE 3

REGRESSION SUMMARY

| Sample | $N_{\rm stars}$ | Technique | $A_0$ | $\sigma$ | $A_1$ | $\sigma$ | $A_2$ | $\sigma$ | $N_{\rm outliers}$ | $r^2$ |
|---|---|---|---|---|---|---|---|---|---|---|
| A ..... | 94 | WLS | −0.26 | 0.36 | 0.042 | 0.005 | 0.062 | 0.018 | ... | 0.400 |
| A ..... | 94 | LS | −0.21 | 0.32 | 0.042 | 0.006 | 0.094 | 0.019 | ... | 0.403 |
| A ..... | 89 | RLS/LMS | 0.04 | 0.29 | 0.038 | 0.005 | 0.105 | 0.017 | 5 | 0.462 |
| B ..... | 109 | WLS | −0.13 | 0.33 | 0.041 | 0.005 | 0.102 | 0.014 | ... | 0.467 |
| B ..... | 109 | LS | −0.12 | 0.29 | 0.042 | 0.005 | 0.119 | 0.015 | ... | 0.494 |
| B ..... | 98 | RLS/LMS | 0.41 | 0.23 | 0.034 | 0.004 | 0.131 | 0.012 | 11 | 0.630 |

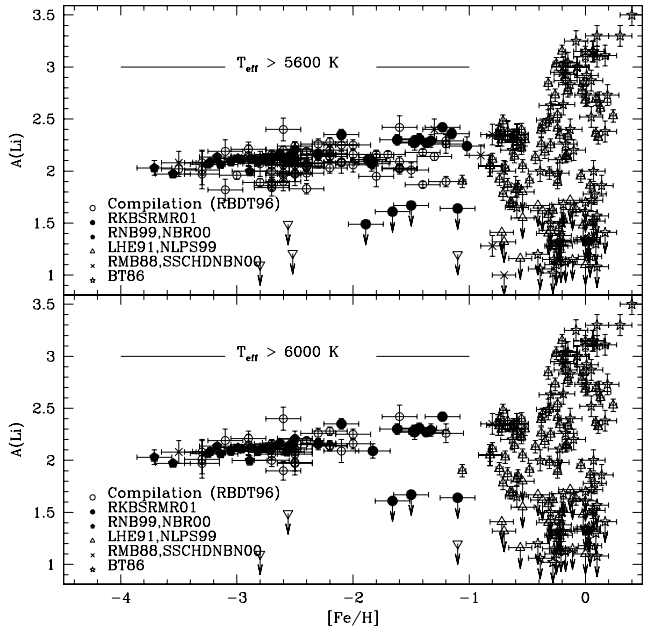


FIG. 6.—*Top panel:* $A$(Li) on [Fe/H] for halo, young disk, and old disk. Data are from Boesgaard & Tripicco (1986), Rebolo et al. (1988), Lambert et al. (1991), Nissen et al. (1999), Spite et al. (2000), the homogenized compilation by Ryan et al. (1996a), and recent data by Ryan et al. (1999) and Norris et al. (2000). The halo stars have $T_{\rm eff} > 5600$ K. *Bottom panel:* As for the top panel, but restricting the halo sample to $T_{\rm eff} > 6000$ K to avoid the (genuine or artificial) $T_{\rm eff}$ dependence.

stars, those having $T_{\rm eff} > 6000$ K. The elimination of cooler stars, for which we derive generally lower Li abundances, results in a narrower trend of $A$(Li) versus [Fe/H]. In the following section we will use this sample to constrain GCE models in an attempt to develop a clearer picture of the evolution of this element.

A recent analysis of BD +00°2058A (King 1999) derives a considerably higher Li abundance for this star, $A(\mathrm{Li}) = 2.53 \pm 0.05$, than we do, $A(\mathrm{Li}) = 2.28 \pm 0.05$ (1 $\sigma$). These differ at the 3.5 $\sigma$ level. The King value implies considerably more Li GCE (at least for the material that constitutes this object) than the measurements in our sample. Because of the significance of this potentially high abundance for the remaining discussion, we examine this difference in greater detail. The basic spectral measurements of the star are in good agreement; we list $W = 37.6 \pm 3.3$ mÅ, whereas King measures $W = 42.3$ mÅ from higher S/N and higher resolving power data, to which we would assign a measurement error of $\sigma_W = 1$ mÅ. These equivalent width measurements differ only at the 1.4 $\sigma$ level, which is quite reasonable, and lead to a difference in $A$(Li) of 0.05 dex. King infers a temperature higher by 96 K (a 1.1 $\sigma$ difference), which induces another 0.06 dex abundance difference in the positive direction. As described previously, Li computations are largely insensitive to the gravity and microturbulence, and we do not expect these differences in our analysis to lead to significant abundance changes. The other major difference in the analyses is the choice of model atmospheres. While our work (Ryan et al. 1996a) is based on R. A. Bell (1983, private communication) models that closely match older R. L. Kurucz (1989, private communication) models, King adopts the overshooting models of Kurucz (1993), which are hotter in the shallower layers. The higher temperatures in these newer models, even for an identical $T_{\rm eff}$, result in weaker lines being computed and hence higher abundances being inferred to match the observations. This accounts for an additional difference of $\simeq 0.11$ dex (see Ryan et al. 1996a, Fig. 2) for Li and accounts at least partially for the higher [Fe/H] derived by King; see Ryan, Norris, & Beers (1996b) for a discussion of model differences in the context of elements other than Li, which show effects at a similar order of magnitude. Through the differences in observed line strength, effective temperature, and choice of model, we are thus able to understand 0.22 dex of the 0.25 dex difference. In view of diminishing returns, we do not endeavor to trace the remaining 0.03 dex difference. As all of the data presented in our current work are on the same $T_{\rm eff}$ and model atmosphere scale as those in the works by Ryan et al. (1996a, 1999), we maintain the data shown in our Table 1, without adjustment. The Li abundance in BD +00°2058A is not, in our view, any more remarkable than the abundances in the rest of the stars at that metallicity; King's (1999) impression, to the contrary, emerged from the comparison of one star analyzed on one system with the bulk of data analyzed on another. We nevertheless acknowledge King's superior data and note that using King's equivalent width measurement on our effective temperature and model atmosphere system would lead to $A(\mathrm{Li}) = 2.33 \pm 0.04$.

Before concluding this section, we draw attention to the four stars in the current survey for which no Li line was detectable. Detection of four extremely Li-deficient objects in a sample of 18 stars, when previous estimates of the frequency of such objects in the halo population was 5% (Norris et al. 1997), is astonishing. These objects are discussed in a companion paper (Ryan et al. 2001) and will be excluded from further discussion in the present work.

## 4. GALACTIC CHEMICAL EVOLUTION OF Li

In this section we compare the observed metallicity dependence of $A$(Li) with several models for GCE, in the hope of gaining a better understanding of the sources of this element. We explicitly assume that halo dwarfs with [Fe/H] $< -1$ and $T_{\rm eff} > 6000$ K have not depleted their prestellar surface abundances in situ. However, the GCE models *do* allow for astration, i.e., the removal of Li from the gas "reservoir" of star formation via its destruction in stars that, at the end of their lives, remix with the interstellar medium (ISM) via winds and/or ejecta. We also assume that the observed abundances apply to pure $^7$Li only, i.e., that any prestellar $^6$Li has been destroyed unless stated otherwise. This could be incorrect for the highest temperature stars in this parameter range but is unlikely to overestimate the $^7$Li abundance by more than 5% (0.02 dex) based on the few $^6$Li detections achieved.

### 4.1. *A Simple, Linear Evolution "Fiducial" Model*

A simple analytic model could assume that postprimordial net production of Li evolved linearly with iron, giving $n(\mathrm{Li}) = n(\mathrm{Li})_p + kn(\mathrm{Fe})$, where $A(\mathrm{Li})_p$ is the primordial abundance and $k = dn(\mathrm{Li})/dn(\mathrm{Fe})$ is the relative rate of Li and Fe nucleosynthesis (assumed in this simple model to be constant). Two boundary conditions fully specify the model: the primordial abundance of Li and the meteoritic abundance. Adopting $A(\mathrm{Li})_p = 2.10$ for the former and $A(\mathrm{Li})_m = 3.30$ for the latter (see Grevesse & Sauval 1998) and using $A(\mathrm{Fe})_\odot = -4.50 + 12.00$ yields $k = 6.31 \times 10^{-5}$, or one Li atom produced (net) for every 16,000 Fe atoms.

Such a linear evolution model ignores all of the details of the physics of nucleosynthesis and stellar life cycles and instead relies on a hypothesized association of Li-producing events with Fe-producing events, be they due to Galactic cosmic-ray (GCR) spallation, the $\nu$-process, or some other.[3] The model is shown in Figure 7*a*, where a remarkable similarity to the data can be seen. The fact that such a simple model gets even close to the observations indicates that the real process(es) responsible for Li production in the halo do indeed follow Fe production almost linearly. However, the mismatch during the evolution of the disk indicates that a more efficient source of Li production relative to iron is required to reproduce the steep $A$(Li)-versus-[Fe/H] trend exhibited by the disk data. We find the elements of such a model in the work by Romano et al. (1999), as discussed below, in particular the "late" synthesis of Li in novae and asymptotic giant branch (AGB) stars.

Changing the evolution assumption to linearity with the $\alpha$-elements, where we adopt $[\alpha/\mathrm{Fe}] = 0.4$ for $[\mathrm{Fe/H}] < -1$ and $[\alpha/\mathrm{Fe}] = -0.4[\mathrm{Fe/H}]$ otherwise, flattens the rate of Li evolution in the disk (where $\alpha$-elements evolve more slowly with respect to iron; this is expected on the basis of the time delay model of chemical evolution, since Fe is mostly produced by SNe Ia whereas $\alpha$-elements are essentially synthesized by SNe II). As a consequence, the Li evolution in the halo phase must be greater in order to reach the meteoritic abundance at $[\mathrm{Fe/H}] = 0$, with the result that the model curve is higher under this scenario, and lithium is clearly overproduced as compared to the observational data.

### 4.2. *The GCE Model of Fields* & Olive (*1999a, 1999b*)

Fields & Olive (1999a, 1999b) developed a GCE model of postprimordial $^7$Li production by GCR spallation and fusion (which also produce $^6$Li, $^9$Be, and $^{10,11}$B) and by supernovae through the $\nu$-process (which also produces $^{11}$B; Woosley et al. 1990). The GCR composition is assumed to scale with the ISM composition, which leads to dominance of the fusion source (as opposed to spallation) during halo star formation (e.g., Steigman & Walker 1992) and linear evolution of the GCR Li contribution with the number of supernovae during this era. The $\nu$-process likewise gives linear evolution with the number of supernovae. The normalizations of these sources are set by the meteoritic abundances; $^9$Be and $^{10}$B set the GCR contribution, and the $^{11}$B unaccounted for by this means fixes the $\nu$-process contribution.

The number of Type II supernovae contributing to the production of Li in the early Galaxy can, in principle, be traced by the abundances of heavier elements. Two possible tracers are oxygen and iron, the former made by hydrostatic burning in the progenitor, the latter formed during the explosive phase, and both expelled during the explosion. However, it is unclear which element is a better tracer of supernova numbers; iron yields are notoriously difficult to calculate because of its dependence on many factors associated with the explosion (e.g., mass cut, neutronization, rotation; Timmes, Woosley, & Weaver 1995; Hix & Thielemann 1996; Hoffman et al. 1999; Nakamura et al. 1999), while observational studies of oxygen have often provided inconsistent results (reviewed by Gratton 2000). The Fields & Olive (1999a, 1999b) models use oxygen as the tracer and utilize in particular the [O/Fe] results of Israelian, García Lopéz, & Rebolo (1998) and Boesgaard et al. (1999).[4]

The linearity of Li nucleosynthesis with the number of supernovae, both for the GCR and $\nu$-process, partially justifies the choice of parameters in the simple linear evolution model described above. The Fields & Olive (1999a, 1999b) model, however, is based on proper physical processes and is shown in Figure 7*b* for $A(\mathrm{Li})_p = 2.04$. Two curves are shown depending on whether the GCE $^6$Li component is preserved or destroyed at the surface. This model was intended to explore Li GCE in Population II stars only and excludes additional stellar production mechanisms that come into play during the evolution of the Galactic disk. For this reason, the appropriate test of the model against the data involves only the stars with $[\mathrm{Fe/H}] < -1$, not the disk stars at higher metallicity that the model does not address. It should also be noted that the model shown was developed prior to the reduction and analysis of the new data presented in this paper (for stars at $[\mathrm{Fe/H}] \sim -1.5$), so the excellent fit of the Fields & Olive (1999a, 1999b) model to these new points is a genuine achievement of the model.

Note that the predictions of the Fields & Olive (1999a, 1999b) model, especially for the more metal-rich stars, depend on the survival fraction of $^6$Li. Where $^6$Li has been measured in stars with $[\mathrm{Fe/H}] \sim -2.4$ (Smith, Lambert, & Nissen 1993, 1998; Cayrel et al. 1999; Hobbs & Thorburn 1994, 1997; C. P. Deliyannis & S. G. Ryan 2001, in preparation), its total fraction is low but nevertheless consistent with the Fields & Olive (1999a, 1999b) model (see Ryan et al. 2000). Bear in mind also that $^6$Li retention is likely to be a function of metallicity, as discussed by Ryan et al. (1999), so the data might be expected to follow the dashed curve at lowest [Fe/H] and the solid curve at higher [Fe/H].

### 4.3. *The GCE Model of Romano et al.* (*1999*)

The Li GCE model by Romano et al. (1999) includes five components: primordial nucleosynthesis, GCR spallation (using the prescription of Lemoine, Vangioni-Flam, & Cassé 1998), supernova nucleosynthesis via the $\nu$-process, AGB star nucleosynthesis via hot-bottom burning and the $^7$Be transport mechanism (Cameron & Fowler 1971; Sackmann & Boothroyd 1992), and novae (José & Hernanz 1998). Of the postprimordial contributions, the $\nu$-process dominated during the halo phase, so much so that Romano et al. (1999) considered a model with the contributions from this process halved to avoid overproduction of Li. AGB stars were found to contribute only for $[\mathrm{Fe/H}] \gtrsim -0.8$, and novae only for $[\mathrm{Fe/H}] \gtrsim -0.5$. Therefore, for halo star evolution only the primordial nucleosynthesis, the $\nu$-process, and GCR processes are significant. These are the same contributions included in the Fields & Olive (1999a,

[3] Parizot & Drury (1999), for example, emphasize that the linear relation between isotopes that emerges from their work is the result of differential *dilution*, rather than accumulation. This model therefore also follows a linear evolution path and provides a very different example of a complex physical model whose outcome can, with the benefit of hindsight, be approximated over the halo epoch by a simple linear relation.

[4] We note that the issue of the correct value of the halo [O/Fe] ratio remains contentious (e.g., Fulbright & Kraft 1999). The 2000 IAU General Assembly had a 1 day joint discussion on this problem.

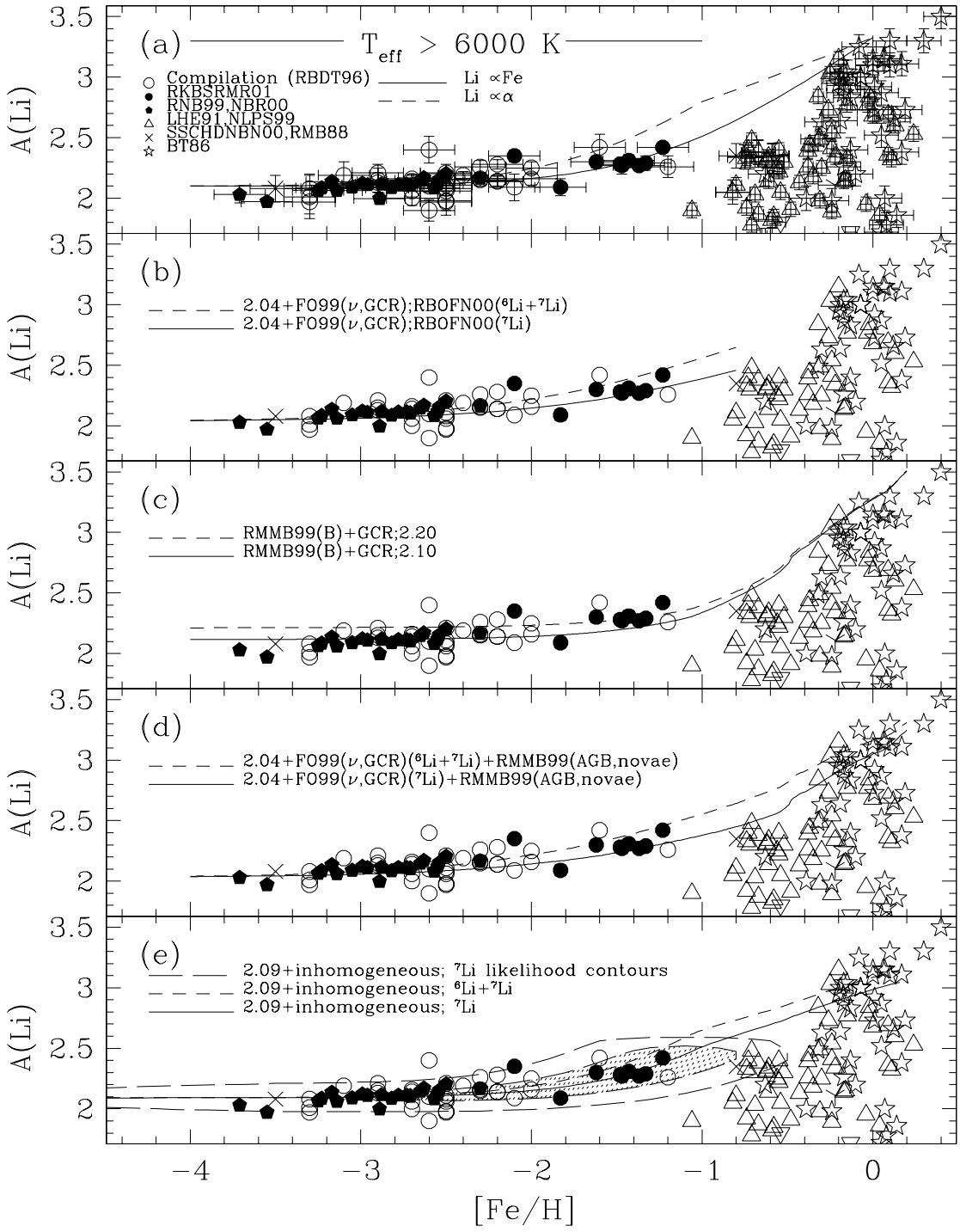


FIG. 7.—Comparison of halo, old disk, and young disk star observations (Fig. 6) with theoretical models. (*a*) Simple two-component model. *Solid curve*: Assumes Li production scales with iron; *dashed curve*: assumes Li production scales with the α-elements. (*b*) Primordial, GCR, and *ν*-process model of Fields & Olive (1999a, 1999b; Ryan et al. 2000). *Solid curve*: $^7$Li only; *dashed curve*: includes $^6$Li. (*c*) Five-component model: primordial, GCR, *ν*-process, AGB star, and novae model of Romano et al. (1999). *Solid curve*: Adopts $A(\mathrm{Li})_p = 2.10$; *dashed curve*: $A(\mathrm{Li})_p = 2.20$. (*d*) Hybrid model using (*b*) plus the AGB star and novae contributions from (*c*). *Solid curve*: $^7$Li only; *dashed curve*: includes $^6$Li. (*e*) Inhomogeneous model. The two long-dashed contour lines, from the inside outward, correspond to the (error-convolved) frequency distribution of long-lived stars of constant probability density $10^{-4}$ and $10^{-8}$ in unit area of $(\Delta[\mathrm{Fe/H}] = 0.1) \times [\Delta A(\mathrm{Li}) = 0.002]$. (The inner contour is shaded for clarity.) *Solid curve*: Evolution of the $^7$Li gas abundance. *Short-dashed curve*: $^6\mathrm{Li} + {}^7\mathrm{Li}$ abundance.

1999b) model, albeit with different normalizations. The considerable contribution of novae and nonnegligible contribution of AGB stars at "late" times of GCE, i.e., for the disk, are promising candidates for the sources required to raise $A$(Li) from the value of the most metal-poor disk stars to the meteoritic one.

In Figure 7*c* we show Romano's model "B" plus their adopted GCR contribution (based on the work of Lemoine

et al. 1998). Their model adopted $A(\mathrm{Li})_p = 2.20$, whereas our data suggest a lower value, so we also show a second model with the primordial value reduced to $A(\mathrm{Li})_p = 2.10$ to fit the most metal-poor stars. The Romano et al. (1999) models provide a very good fit to the disk star data and indicate that the substantial contribution of novae at late times may indeed be the requirement to account for the steep evolution of $A$(Li) in the disk. The Romano et al. (1999) models fit the most metal-poor halo and disk data very well but underpredict the abundances measured in the present work for high-metallicity halo stars by $\simeq 0.08$ dex. This difference could be due to a metallicity-dependent systematic error in the color–effective temperature calibration, if that error changes by 100 K over the interval from [Fe/H] $= -1.5$ to $-3.0$. An error of this magnitude is possible but has not been identified. If, on the other hand, the derived abundances are reliable, then one would infer that the rate of Li evolution in the halo phase of the model appears to be somewhat low, as a result of the use of the Lemoine et al. (1998) Li absolute yields from GCRs that would then appear to underestimate GCR Li production during the halo phase.

### 4.4. *A Hybrid Model*

We found above that the Fields & Olive (1999a, 1999b) model fit the halo evolution of the Galaxy very well, while the Romano et al. (1999) model included the steep evolution required during the disk phase. In this subsection we examine a combination of the two, using the primordial, GCR, and $\nu$-process calculations of Fields & Olive (1999a, 1999b) and adding the AGB star and novae contributions computed by Romano et al. (1999) for the disk phase. This hybrid replaces the GCR prescription of Lemoine et al. (1998) and the $\nu$-process yields of Woosley & Weaver (1995) adopted by Romano et al. (1999) with the ones of Fields & Olive (1999a, 1999b) described above.

We recognize that combining these model results is not self-consistent, in that the full GCE calculation including astration was applied by Romano et al. (1999) on the basis of the components *they* included, and not on the basis of the Fields & Olive (1999a, 1999b) components, which we now seek to substitute. Clearly, a self-consistent recalculation is desirable. However, astration appears to be a fairly minor factor compared with the source terms, at least up to [Fe/H] $= -0.6$, judging by the minor impact on the survival fraction of primordial Li in the Matteucci, Romano, & Molaro (1999, Fig. 9*a*) calculations and in the Fields & Olive model (Ryan et al. 2000, Fig. 1). Consequently, we regard our present hybrid approach as a valuable initial investigation of the effect of combining these sources.

The hybrid model is shown in Figure 7*d*. The Fields & Olive GCR$+\nu$ component is clearly weaker than that in Figure 7*c* because the hybrid model does not reach the meteoritic value, but it does improve the fit to the halo and old disk data. Although the young disk data are not so well reproduced, the appearance of nova and AGB star nucleosynthesis in the calculations of Romano et al. (1999) coincides with the observed steepening of disk star Li evolution, and the novae source term is regarded as quite uncertain. As emphasized by the fiducial linear evolution model (Fig. 7*a*), Li must evolve considerably faster relative to iron during formation of young disk stars to reproduce the data. Even though none of the models, on their own, produce a *perfect* fit to *all* of the metal-poor halo, metal-rich halo, old disk, and young disk data, the key features of the hybrid of Romano et al. (1999) and Fields & Olive (1999a, 1999b) models are in very good accord with the observations and strongly suggest that these models are viable (though not necessarily uniquely so; see below).

### 4.5. *The Inhomogeneous GCE Model of Suzuki et al. (1999)*

Several recent models of GCE propose that very metal-deficient stars were formed in individual supernova remnant (SNR) shells in the Galactic halo during its early epochs before the gas of the ISM was well mixed and that their abundance patterns reflect the contributions of elements synthesized in *single* SN IIe events (Ryan, Norris, & Bessell 1991; Audouze & Silk 1995; McWilliam et al. 1995; Ryan et al. 1996b). Even for stars of similar iron content, the observed abundances of several $r$-process elements in these stars show remarkable scatter (Gilroy et al. 1988; Ryan et al. 1991, 1996b; McWilliam et al. 1995). This scatter is presumed to arise from the inhomogeneous evolution of the early Galactic halo, in particular the finite extent of SNRs responsible for early enrichment of the proto-Galactic gas (Ryan et al. 1996b). This framework casts doubt on the applicability of simple one-zone models, such as those discussed in the previous subsections, for describing the chemical evolution of the Galaxy. Lithium must also be included in any paradigm shift of this sort. Tsujimoto, Shigeyama, & Yoshii (1999; see also Argast et al. 2000) have proposed an SN-induced chemical evolution model that takes account of inhomogeneous circumstances arising from the stochastic nature of star formation processes triggered by SN explosions. Their model can explain the scatter seen in the Eu abundance and can be applied to other elements, e.g., iron, as well.

An extension of the inhomogeneous model to investigate the evolution of the light elements Be and B, which are mainly produced by nuclear reactions involving GCRs, has been developed by Suzuki et al. (1999). They proposed a new scenario, that GCRs originate from both the SN ejecta and the swept-up ISM accelerated by the shock formed in the SNR shell, and demonstrated that this model reproduces the observed trends of Be and B very well. The GCRs accelerated by SN shocks propagate through the inhomogeneous Galactic halo to interact with both the ambient ISM and the gas in SNR shells, producing Be and B. Their model exhibits a linear increase of log (BeB) $\propto$ [Fe/H] quite naturally. They suggested, for the first time, that there might be expected a good correlation between time since the initiation of star formation in the early Galaxy and $^6$LiBeB abundances, even for low-metallicity stars [Fe/H] $\leq -2$, an epoch when no unique time-metallicity relation is expected to exist for heavier elements that are more affected by the inhomogeneous nature of the early Galactic halo (Suzuki & Yoshii 2001; Beers, Suzuki, & Yoshii 2000). The implications for the chemical evolution of Li should therefore be investigated in this inhomogeneous GCE model.

In the inhomogeneous model presented here, contributions from five components are included, as in the model of Romano et al. (1999): primordial nucleosynthesis, GCR spallative and $\alpha + \alpha$ fusion reactions, SN nucleosynthesis via the $\nu$-process (Woosley & Weaver 1995), AGB star nucleosynthesis (Forestini & Charbonnel 1997), and nova nucleosynthesis (José & Hernanz 1998). The predicted $^7$Li

yields of Woosley & Weaver (1995) for different SN progenitor masses are used for the $\nu$-process, but the absolute values are reduced by a factor of 5 in order to match the observed $^{11}B/^{10}B$ ratio. Note that the same model setup is applied to all light elements $^{6,7}Li$, $^{9}Be$, and $^{10,11}B$ without any adjustable parameter for each element. To extend their model smoothly to later times, evolution of the disk ([Fe/H] $> -1.0$) assumes a simple one-zone chemical evolution model with infall (e.g., Pagel 1997).

Figure 7*e* displays the result obtained in our model calculation. The primordial lithium abundance is chosen to be $A(\mathrm{Li})_p = 2.09$, derived from likelihood analysis (Suzuki et al. 2000) by comparing the theoretical frequency distribution of stars with recent accurate observations by Ryan et al. (1999). The frequency distribution is convolved with a Gaussian having $\sigma = 0.03$ dex for $A$(Li) and $\sigma = 0.15$ dex for [Fe/H], in order to compare with the observed data directly. The long-dashed contours indicate the probability densities of the predicted stellar distribution of $^{7}Li$ in the Galactic halo. The solid curve in the center represents the average trend of the evolution of $^{7}Li$ versus Fe; the short-dashed curve gives the total $^{6}Li + {}^{7}Li$ for when $^{6}Li$ is preserved. The model accounts for the observed halo data very well. Note that a clear departure of Li from the primordial abundance, at [Fe/H] $\lesssim -3$, toward higher metallicity, [Fe/H] $\sim -1$, is apparent, supporting the contention that the observed gradient with [Fe/H] is real. The source of the low-abundance slope is mainly due to Li GCR production, at first ([Fe/H] $< -2$) from the $\alpha + \alpha$ fusion reactions, and later also from spallation reactions as the CNO abundance in the ISM increases. The contribution from the $\nu$-process of SNe is less than 10% of the total postprimordial Li production for the halo phase. Since the predicted increasing trend of Li is greater in stars with metallicity $-2 \leq$ [Fe/H] $\leq -1$ than for more metal-poor stars, additional observations of turnoff dwarfs in this metallicity region would help measure the gradient more precisely. They are also needed to identify uncertain contributions from AGB and novae nucleosynthesis in the old disk phase, where the model slightly overproduces the data.

### 4.6. *Discussion of GCE Models of* Li *and Future Directions*

We noted at the outset of this discussion that, at first sight, there are few *major* differences between the evolutionary trends in the models presented above. The models shown in Figures 7*a*, 7*c*, and 7*e*, for example, have quite different underlying assumptions but predict very similar evolution of Li during the halo phase, especially when the error bars on the observations are taken into account. The reason is that these three models all have mechanisms that are linear with Fe; the underlying assumptions and parameter sets are different, but the proportionality is the same. This highlights a degeneracy in attempts to find the "best" model by comparisons with imperfect data; models based on quite different propositions give rise to very similar GCE histories. The major differences between models arise during the disk phase, which is also where Li evolution is greatest and Li abundances are more easily measured. However, because of the considerable changes in the sources and sinks of Li that operate throughout the course of Galactic history, one must not be fooled into discarding a particular model for halo evolution based on the failure of its disk component, for example. Some of the more subtle differences between the models have already been discussed, but we note the following before concluding.

Of the models presented above, those in Figures 7*c*–7*e* include both halo and disk sources. None provide a perfect match to both Galactic components. All, of course, are "fixed" to the data for the most metal-poor halo stars through the choice of the primordial value. The Romano et al. (1999) model provides a good match to the metal-poor disk and meteoritic values but does not exhibit sufficient Li evolution during the halo phase and overpredicts the Li abundance at [Fe/H] $\simeq -0.5$; the observations show a later onset for high Li production. The hybrid model, which combines the halo evolution of Fields & Olive (1999a, 1999b) with the Romano et al. (1999) disk results, provides a better fit to the metal-rich halo and metal-poor disk data up to and including the stage [Fe/H] $\simeq -0.5$ but does not provide sufficient Li production during the later stages of the disk and fails to reach the meteoritic value. The inhomogeneous model of Suzuki et al. (1999) likewise produces a good fit to the halo data within a quite different framework, but the one-zone disk calculation to which it is connected is inadequate. As the mismatch between the disk observations and the simple fiducial model emphasizes, the efficiency of Li production relative to iron must increase substantially during the late phase of disk evolution if the Li enhancement at [Fe/H] $> -0.5$ is to be reproduced.

The models have emphasized the importance of the GCR contribution to Li during halo evolution. The Fields & Olive (1999a, 1999b) and Suzuki et al. (1999) models have both assumed a traditional energy spectrum for the $\sim$100–1000 MeV cosmic rays, but one should also be aware that a quite different class of energetic particles may play an important role. Several authors have examined the possible role of a shock-accelerated low-energy component (LEC) that dominates the particle flux at a few times 10 MeV, the threshold for Li production (e.g., Ramaty, Kozlovsky, & Lingenfelter 1996; Vangioni-Flam et al. 1998). Ramaty et al. (1996) and Lemoine et al. (1998; also adopted by Romano et al. 1999), for example, conclude that the solar/meteoritic light-element abundances can be best fitted with contributions from both the GCR and LEC components in ratios 1:3 and 1:1, respectively. Moreover, Vangioni-Flam et al. (1998, 1999) show that the LEC can dominate light-element production during the halo phase, the traditional GCR contribution becoming significant only during evolution of the disk. A better understanding of this component is essential to obtaining correct models of Li evolution throughout Galactic history. As the Vangioni-Flam et al. (1998) LEC models invoke acceleration in superbubbles (e.g., Parizot & Drury 1999), treatment of this mechanism in an *inhomogeneous* halo environment (a la Suzuki et al. 1999) would also be a valuable undertaking.

Another remarkable feature of the models shown in Figure 7 is that the range we see in $A$(Li) values for new observations at [Fe/H] $> -2$ is consistent with the modeled evolutionary rates of Li and does not require a spread in Li about the trend in excess of that due to measurement errors alone. The one exception among our new observations is CD $-30°18140$, which sits above the curves. It will be interesting to see whether future investigations of this object, including a detailed stellar atmosphere analysis, confirm it as lying above the curves.

Note that we have avoided any discussion of *time* rates of evolution; the mismatch with the fiducial model emphasizes

that Li production relative to *iron* must increase. The challenge for astronomers is to identify the source of that Li. The models discussed above have so far excluded a recently recognized source of Li, namely, cool-bottom processing in low-mass red giants (e.g., Sackmann & Boothroyd 1999). This has been used to explain the observations of Li-rich stars in this phase of evolution (e.g., Charbonnel & Balachandran 2000; Drake, de la Reza, & da Silva 2000; Gregorio-Hetem et al. 2000).[5] The contributions of these stars to the overall chemical evolution of the Galaxy are not yet known, but it is clear by their low mass that they will contribute only late in the evolution of the system. We might speculate, therefore, that such objects could be significant contributors to disk evolution that will provide the required higher efficiency of Li production relative to iron at [Fe/H] $> -0.5$.

## 5. CONCLUSIONS

We have measured the Li abundances of 18 stars with $-2 <$ [Fe/H] $< -1$ and $6000 < T_{\rm eff} < 6400$ K, populating a previously poorly sampled region of the $T_{\rm eff}$-[Fe/H] plane. Of these, four proved to be highly Li deficient (and are discussed in the companion paper), with $A(\rm Li) < 1.7$. The remaining 14 were found to conform to the same trends of $A$(Li) with $T_{\rm eff}$ and [Fe/H] identified earlier by Ryan et al. (1996a), removing any doubts that the results of that study were affected by the selection biases inherited in the observational samples.

It is unclear whether the $T_{\rm eff}$ trend we have identified is intrinsic or due to the photometric effective temperature scales used, but this uncertainty was largely circumvented by restricting our attention to stars in a narrow $T_{\rm eff}$ range by excluding those with $T_{\rm eff} < 6000$ K. This subsample of turnoff halo stars, supplemented with objects from previous studies occupying the same temperature range, revealed a *significant increase* of $A$(Li) over the metallicity range of the halo, from $A(\rm Li) = 2.10$ at [Fe/H] $= -3.5$ to $A(\rm Li) = 2.40$ at [Fe/H] $= -1.0$.

We examined various GCE models in an attempt to understand the halo and disk phases of Li production and showed, with a simple linear evolution model, that the net Li production rate relative to iron must increase substantially during young disk evolution. A very satisfactory match to the halo and old disk data was found in the three-component (primordial, GCR, and $\nu$-process) model of Fields & Olive (1999a, 1999b; Ryan et al. 2000). The additional sources of stellar nucleosynthesis in the young disk ([Fe/H] $> -0.5$) are well represented by the models of Romano et al. (1999), whose main contributors are novae, and to a lesser extent, AGB stars. A hybrid of the two models provided the best current match to the halo and disk data together. In addition, a new model of halo GCE in an inhomogeneous framework, extending the work of Suzuki et al. (1999), was presented that was equally capable of modeling the halo data.

While none of these models present a perfect fit to all epochs of Galactic evolution, the match between the models and data is sufficiently good to believe that the models are viable, albeit not uniquely so. The primary remaining challenge is to reproduce the efficient production of Li during late stages of disk evolution. A simple fiducial model demonstrates that Li production relative to iron production increases significantly at [Fe/H] $> -0.5$. The disk model of Romano et al. (1999) currently comes closest to predicting this, but we also speculate that the recently identified cool-bottom processing (production) of Li in low-mass red giants (Sackmann & Boothroyd 1999) may provide a late-appearing source of Li without attendant Fe production.

The authors gratefully acknowledge the support for this project given by the Australian Time Assignment Committee (ATAC) and Panel for the Allocation of Telescope Time (PATT) of the AAT and WHT, respectively, and for practical support given by the staff of these facilities. T. C. B. acknowledges partial support from NSF grant AST 95-29454 and, along with S. G. R., wishes to thank the IAU for travel supplement grants that enabled them to attend IAU Symposium 198, where discussions related to this work were held.

[5] The high Li abundance found in the C-rich star CS 22898-027 (Thorburn & Beers 1992) may reflect material transferred from a giant companion. However, the presence of *s*-process enhancements in this particular object (McWilliam et al. 1995) suggests contamination from an AGB rather than a red giant branch (RGB) former primary.

# APPENDIX A

The existence, or not, of correlations between the estimated abundance, $A$(Li), and the physical parameters, $T_{\rm eff}$ and [Fe/H], individually or in a multiple regression approach, has been the subject of a number of recent papers. For transparency, we include our complete regression results for the samples discussed in this paper.

## A1. DATA SAMPLES AND METHODOLOGY

The data sets we consider are as follows:

Sample A: The values of $A$(Li), $T_{\rm eff}$, and [Fe/H] published by Ryan et al. (1996a). (The regressions published by Ryan et al. 1996a were based on a penultimate version of the data, prior to final updates for a few stars. We have also changed our approach for carrying out the weighted least-squares analysis as discussed below, so our present values, though differing little, supersede those reported previously.)

Sample B: Our estimates of $A$(Li), $T_{\rm eff}$, and [Fe/H] presented in this paper, plus the data from Ryan et al. (1996a, 1999), Norris et al. (2000), and Spite et al. (2000). Where a star appears twice, the most recent data have been used. Stars with only upper limits on $A$(Li) have been excluded.

TABLE 4

DETAILED REGRESSION RESULTS

| Sample (1) | $N_{stars}$ (2) | Model (3) | $T_{cut}$ (4) | Technique (5) | $A_0$ ($\sigma$) (6) | $A_1$ ($\sigma$) (7) | $A_2$ ($\sigma$) (8) | $R^2$ (9) | $r(T_{eff}, [Fe/H])$ (10) |
|---|---|---|---|---|---|---|---|---|---|
| A ..... | 94 | 1 | All | WLS | −0.027 (0.376) | 0.035 (0.005) | ... | 0.324 | ... |
| A ..... | 94 | 1 | All | LS | 0.180 (0.352) | 0.032 (0.006) | ... | 0.244 | ... |
| A ..... | 89 | 1 | All | RLS/LMS | −0.168 (0.323) | 0.037 (0.005) | ... | 0.362 | ... |
| A ..... | 81 | 1 | >5800 | WLS | 0.474 (0.465) | 0.027 (0.007) | ... | 0.166 | ... |
| A ..... | 81 | 1 | >5800 | LS | 0.501 (0.489) | 0.027 (0.008) | ... | 0.121 | ... |
| A ..... | 79 | 1 | >5800 | RLS/LMS | 0.319 (0.465) | 0.029 (0.008) | ... | 0.163 | ... |
| A ..... | 54 | 1 | >6000 | WLS | 0.261 (0.735) | 0.031 (0.011) | ... | 0.122 | ... |
| A ..... | 54 | 1 | >6000 | LS | 0.025 (0.803) | 0.034 (0.013) | ... | 0.117 | ... |
| A ..... | 52 | 1 | >6000 | RLS/LMS | −0.110 (0.733) | 0.037 (0.012) | ... | 0.159 | ... |
| A ..... | 94 | 2 | All | WLS | 2.131 (0.244) | ... | 0.013 (0.022) | 0.004 | ... |
| A ..... | 94 | 2 | All | LS | 2.196 (0.056) | ... | 0.041 (0.022) | 0.036 | ... |
| A ..... | 91 | 2 | All | RLS/LMS | 2.256 (0.055) | ... | 0.064 (0.022) | 0.090 | ... |
| A ..... | 81 | 2 | >5800 | WLS | 2.125 (0.235) | ... | 0.002 (0.021) | 0.000 | ... |
| A ..... | 81 | 2 | >5800 | LS | 2.239 (0.056) | ... | 0.050 (0.022) | 0.062 | ... |
| A ..... | 78 | 2 | >5800 | RLS/LMS | 2.294 (0.052) | ... | 0.074 (0.020) | 0.145 | ... |
| A ..... | 54 | 2 | >6000 | WLS | 2.374 (0.232) | ... | 0.088 (0.028) | 0.160 | ... |
| A ..... | 54 | 2 | >6000 | LS | 2.393 (0.075) | ... | 0.098 (0.028) | 0.192 | ... |
| A ..... | 52 | 2 | >6000 | RLS/LMS | 2.423 (0.068) | ... | 0.113 (0.025) | 0.282 | ... |
| A ..... | 94 | 3 | All | WLS | −0.263 (0.363) | 0.042 (0.005) | 0.062 (0.018) | 0.400 | 0.35 |
| A ..... | 94 | 3 | All | LS | −0.205 (0.324) | 0.042 (0.006) | 0.094 (0.019) | 0.403 | 0.40 |
| A ..... | 89 | 3 | All | RLS/LMS | 0.040 (0.289) | 0.038 (0.005) | 0.105 (0.017) | 0.462 | 0.33 |
| A ..... | 81 | 3 | >5800 | WLS | −0.072 (0.491) | 0.039 (0.008) | 0.059 (0.022) | 0.238 | 0.53 |
| A ..... | 81 | 3 | >5800 | LS | −0.233 (0.460) | 0.043 (0.008) | 0.099 (0.021) | 0.432 | 0.32 |
| A ..... | 77 | 3 | >5800 | RLS/LMS | 0.155 (0.414) | 0.036 (0.007) | 0.100 (0.019) | 0.526 | 0.41 |
| A ..... | 54 | 3 | >6000 | WLS | −0.068 (0.636) | 0.041 (0.010) | 0.112 (0.025) | 0.364 | 0.23 |
| A ..... | 54 | 3 | >6000 | LS | −0.438 (0.675) | 0.047 (0.011) | 0.122 (0.025) | 0.401 | 0.34 |
| A ..... | 50 | 3 | >6000 | RLS/LMS | −0.176 (0.528) | 0.043 (0.009) | 0.123 (0.020) | 0.530 | 0.19 |
| B ..... | 109 | 1 | All | WLS | 0.386 (0.393) | 0.029 (0.005) | ... | 0.204 | ... |
| B ..... | 109 | 1 | All | LS | 0.331 (0.363) | 0.029 (0.006) | ... | 0.182 | ... |
| B ..... | 104 | 1 | All | RLS/LMS | 0.654 (0.338) | 0.024 (0.006) | ... | 0.153 | ... |
| B ..... | 96 | 1 | >5800 | WLS | 1.106 (0.482) | 0.017 (0.007) | ... | 0.058 | ... |
| B ..... | 96 | 1 | >5800 | LS | 0.973 (0.499) | 0.019 (0.008) | ... | 0.054 | ... |
| B ..... | 88 | 1 | >5800 | RLS/LMS | 1.937 (0.431) | 0.003 (0.007) | ... | 0.002 | ... |
| B ..... | 65 | 1 | >6000 | WLS | 2.100 (0.826) | 0.001 (0.013) | ... | 0.000 | ... |
| B ..... | 65 | 1 | >6000 | LS | 1.460 (0.832) | 0.011 (0.014) | ... | 0.011 | ... |
| B ..... | 60 | 1 | >6000 | RLS/LMS | 2.551 (0.728) | −0.007 (0.012) | ... | 0.006 | ... |
| B ..... | 109 | 2 | All | WLS | 2.259 (0.229) | ... | 0.059 (0.017) | 0.100 | ... |
| B ..... | 109 | 2 | All | LS | 2.303 (0.044) | ... | 0.082 (0.018) | 0.162 | ... |
| B ..... | 99 | 2 | All | RLS/LMS | 2.304 (0.036) | ... | 0.080 (0.015) | 0.237 | ... |
| B ..... | 96 | 2 | >5800 | WLS | 2.272 (0.218) | ... | 0.058 (0.016) | 0.126 | ... |
| B ..... | 96 | 2 | >5800 | LS | 2.334 (0.041) | ... | 0.087 (0.017) | 0.224 | ... |
| B ..... | 88 | 2 | >5800 | RLS/LMS | 2.387 (0.032) | ... | 0.103 (0.013) | 0.418 | ... |
| B ..... | 65 | 2 | >6000 | WLS | 2.493 (0.165) | ... | 0.135 (0.013) | 0.614 | ... |
| B ..... | 65 | 2 | >6000 | LS | 2.463 (0.045) | ... | 0.126 (0.017) | 0.458 | ... |
| B ..... | 58 | 2 | >6000 | RLS/LMS | 2.416 (0.033) | ... | 0.109 (0.012) | 0.575 | ... |
| B ..... | 109 | 3 | All | WLS | −0.130 (0.331) | 0.041 (0.005) | 0.102 (0.014) | 0.467 | 0.36 |
| B ..... | 109 | 3 | All | LS | −0.120 (0.293) | 0.042 (0.005) | 0.119 (0.015) | 0.494 | 0.30 |
| B ..... | 98 | 3 | All | RLS/LMS | 0.406 (0.234) | 0.034 (0.004) | 0.131 (0.012) | 0.630 | 0.26 |
| B ..... | 96 | 3 | >5800 | WLS | 0.026 (0.433) | 0.039 (0.007) | 0.103 (0.016) | 0.356 | 0.49 |
| B ..... | 96 | 3 | >5800 | LS | −0.048 (0.410) | 0.041 (0.007) | 0.123 (0.016) | 0.432 | 0.39 |
| B ..... | 89 | 3 | >5800 | RLS/LMS | 0.670 (0.338) | 0.029 (0.006) | 0.123 (0.013) | 0.526 | 0.38 |
| B ..... | 65 | 3 | >6000 | WLS | 1.402 (0.500) | 0.018 (0.008) | 0.141 (0.013) | 0.645 | 0.21 |
| B ..... | 65 | 3 | >6000 | LS | 0.366 (0.578) | 0.035 (0.009) | 0.144 (0.017) | 0.554 | 0.29 |
| B ..... | 60 | 3 | >6000 | RLS/LMS | 0.747 (0.437) | 0.028 (0.007) | 0.136 (0.013) | 0.662 | 0.27 |
| C ..... | 41 | 1 | All | WLS | −1.591 (0.707) | 0.063 (0.011) | ... | 0.476 | ... |
| C ..... | 41 | 1 | All | LS | −0.890 (0.548) | 0.051 (0.009) | ... | 0.444 | ... |
| C ..... | 41 | 1 | All | RLS/LMS | −0.890 (0.548) | 0.051 (0.009) | ... | 0.444 | ... |
| C ..... | 35 | 1 | >5800 | WLS | −2.026 (0.836) | 0.070 (0.013) | ... | 0.481 | ... |
| C ..... | 35 | 1 | >5800 | LS | −1.028 (0.716) | 0.053 (0.012) | ... | 0.380 | ... |
| C ..... | 35 | 1 | >5800 | RLS/LMS | −1.028 (0.716) | 0.053 (0.012) | ... | 0.380 | ... |
| C ..... | 41 | 2 | All | WLS | 2.190 (0.457) | ... | 0.022 (0.062) | 0.003 | ... |
| C ..... | 41 | 2 | All | LS | 2.284 (0.100) | ... | 0.068 (0.058) | 0.034 | ... |
| C ..... | 39 | 2 | All | RLS/LMS | 2.395 (0.089) | ... | 0.123 (0.050) | 0.138 | ... |

TABLE 4—*Continued*

| Sample (1) | $N_{stars}$ (2) | Model (3) | $T_{cut}$ (4) | Technique (5) | $A_0$ ($\sigma$) (6) | $A_1$ ($\sigma$) (7) | $A_2$ ($\sigma$) (8) | $R^2$ (9) | $r(T_{eff}$, [Fe/H]) (10) |
|---|---|---|---|---|---|---|---|---|---|
| C ..... | 35 | 2 | >5800 | WLS | 2.229 (0.500) | ... | 0.039 (0.068) | 0.010 | ... |
| C ..... | 35 | 2 | >5800 | LS | 2.329 (0.101) | ... | 0.083 (0.059) | 0.056 | ... |
| C ..... | 34 | 2 | >5800 | RLS/LMS | 2.378 (0.090) | ... | 0.106 (0.053) | 0.112 | ... |
| C ..... | 41 | 3 | All | WLS | −1.570 (0.708) | 0.064 (0.011) | 0.045 (0.045) | 0.489 | 0.09 |
| C ..... | 41 | 3 | All | LS | −0.772 (0.544) | 0.051 (0.009) | 0.066 (0.043) | 0.477 | 0.01 |
| C ..... | 39 | 3 | All | RLS/LMS | −0.137 (0.515) | 0.042 (0.008) | 0.103 (0.040) | 0.488 | 0.10 |
| C ..... | 35 | 3 | >5800 | WLS | −2.189 (0.799) | 0.076 (0.012) | 0.101 (0.048) | 0.545 | 0.21 |
| C ..... | 35 | 3 | >5800 | LS | −1.107 (0.658) | 0.058 (0.011) | 0.119 (0.045) | 0.493 | 0.16 |
| C ..... | 33 | 3 | >5800 | RLS/LMS | −1.030 (0.575) | 0.058 (0.010) | 0.157 (0.038) | 0.604 | 0.18 |

Sample C: The sample of "metal-rich" stars shown in Figure 5.

The models we consider are the following:

Model 1: $A(\mathrm{Li}) = A_0 + A_1\, T_{\mathrm{eff}}/100$.
Model 2: $A(\mathrm{Li}) = A_0 + A_2[\mathrm{Fe/H}]$.
Model 3: $A(\mathrm{Li}) = A_0 + A_1\, T_{\mathrm{eff}}/100 + A_2[\mathrm{Fe/H}]$.

The regression approaches we utilize are the following:
Technique 1: A weighted least-squares (WLS) approach, wherein the regression is weighted by taking into account the reported statistical error in $A$(Li). In Ryan et al. (1996a) we made use of the routines published in Bevington (1969). In the present application, we choose to employ a different set of routines, those given in the program SYSTAT 9.0 and described in Wilkinson, Blank, & Gruber (1996). These approaches, and hence their results, are slightly different, in that the Bevington routines obtain predicted errors on the regression coefficients that are, in general, a factor of 2–3 lower than those reported by SYSTAT 9.0 (although the derived coefficients are essentially identical). This occurs because the error estimates from Bevington routines do not explicitly take into account the residuals of the points from the derived regression lines but rather assume that the statistical errors fully reflect the expected level of error, which may not be the case for such a diverse data set.
Technique 2: A standard least-squares (LS) approach, which does not take into account the statistical errors on $A$(Li), as obtained by SYSTAT 9.0.
Technique 3: A reweighted least-squares (RLS/LMS) approach based on the least median of squares method of Rousseeuw & Leroy (1987). This approach implements an objective identification of outliers based on deviations from a resistant regression fit (using LMS) obtained from multiple resamples of the data. Once identified, these outliers are removed and a standard (unweighted) least-squares method is applied to the surviving data. This technique makes use of the code provided by Dallal (1991).

### A2. REGRESSION RESULTS

The results for these regressions are summarized in Table 4. Column (1) identifies the sample under consideration. Column (2) lists the number of stars in each sample. Column (3) provides the regression model that is reported. Column (4) lists alternative cuts on effective temperature. Column (5) indicates the regression technique that is applied. Columns (6)–(8) list the derived regression coefficients and their 1 $\sigma$ standard errors. Column (9) is the coefficient of determination, $R^2$, which quantifies the amount of variation of $A$(Li) that can be accounted for by the regression model under consideration (note, $0 \leq R^2 \leq 1$). Column (10) lists, for the bivariate regressions (model 3), the Pearson correlation coefficients between the independent variables $T_{\mathrm{eff}}$ and [Fe/H] obtained by the technique under consideration and is one indication of the presence of possible collinearity between the predictor variables. We consider the results for each of our samples in turn.

### A3. SAMPLE A

As was the case in Ryan et al. (1996a), we identify a significant correlation with effective temperature (considered in isolation: model 1) for the case in which stars of the full range of $T_{\mathrm{eff}}$ values are considered. The significance of the correlation coefficient $A_1$ decreases, as expected, when more aggressive cuts on the lower limit of effective temperatures are made. However, it is illuminating that the size of the coefficient remains roughly constant, on the order of $A_1 \sim 0.03$–$0.035$ dex per 100 K for the different temperature regimes. This suggests that the presence of a temperature-related correlation is not crucially dependent on the inclusion or exclusion of $A$(Li) estimates for stars near the lower limits, where concerns about the possible depletion of surface Li abundance are presently thought to have their greatest effect.

When metallicity is considered in isolation (model 2), we find that the correlation coefficient $A_2$ is small, and not significant, for the full sample A and the subset of sample A with $T_{\mathrm{cut}} > 5800$ K. However, all three of the regression techniques return a significant correlation of $A$(Li) with [Fe/H], roughly $A_2 = 0.10$ dex per dex, when the subsample of stars with $T_{\mathrm{eff}} > 6000$ K is considered. This is an indication that a bivariate fit is required.

For the case of the bivariate regression model (model 3), we note that, as in Ryan et al. (1996a), significant coefficients on both $T_{\mathrm{eff}}$ and [Fe/H] are returned when the full range of temperatures is considered, with a slightly decreasing significance as more aggressive cuts on temperature are considered. It is interesting to note that, for all temperature cuts, the coefficient of

determination indicates that between 25% and 55% of the observed variation in $A$(Li) in the sample can be accounted for by the regression models, which is much higher than seen for the case of either variable considered in isolation.

### A4. SAMPLE B

The application of the above approaches to our expanded and refined sample of stars shows some interesting differences as compared to the published sample of Ryan et al. (1996a).

For model 1, the significance of the coefficient on temperature, $A_1$, drops somewhat compared to sample A when stars of all temperatures are included. For the cuts in temperature, $T_{\rm eff} > 6000$ K and $T_{\rm eff} > 5800$ K, $A_1$ becomes nonsignificant, a fact also revealed from inspection of the coefficients of determination. Nevertheless, the value of the *significant* correlation, obtained for the subsample including stars of all temperatures, is of the same order of magnitude, $A_1 \sim 0.03$ dex per 100 K, as was found for the Ryan et al. (1996a) data set.

For model 2, the significance of the coefficient on [Fe/H], $A_2$, is markedly higher than obtained from the application of this model to sample A above, even when the temperature cuts are applied. Similarly, the coefficients of determination are higher as well. This reflects the fact that sample B includes stars of a wider range in abundance than sample A and also that the errors in estimated $A$(Li) have been substantially reduced for a number of the lowest metallicity stars from the work of Ryan et al. (1999). The value of $A_2$ increases from $A_2 \sim 0.07$ dex per dex to $A_2 \sim 0.12$ dex per dex as one considers progressively more aggressive cuts on temperature. For stars with $T_{\rm eff} > 6000$ K, the coefficient of determination rises to $R^2 \sim 0.5$–$0.6$, indicating that more than 50% of the variation in $A$(Li) is accounted for by this model.

For model 3, which we consider the most appropriate, the significance of both of the coefficients $A_1$ and $A_2$ remains high, and the coefficients of determination are clearly much higher than obtained for sample A above. The correlation coefficients between the $T_{\rm eff}$ and [Fe/H] variables have decreased somewhat for the subsample that includes stars of all temperatures but are roughly similar to those obtained previously for the two temperature cuts. This result indicates that we are making progress with respect to reducing the possible influence of collinearity in the predictor variables but that further work remains: a doubling or tripling of the number of stars with available Li measurements in the metallicity range $-2 \leq$ [Fe/H] $\leq -1$ would be most helpful.

### A5. SAMPLE C

For the "metal-rich" stars that comprise this sample, the regression coefficient on temperature obtained for model 1 is both larger, on the order of $A_1 \sim 0.05$–$0.07$ dex per 100 K, and markedly more significant (note the associated dramatic rise in the values of the coefficients of determination) than was found for either sample A or sample B considered above. The opposite statement can be made concerning the coefficients on [Fe/H], $A_2$, which have decreased to nonsignificance in this subsample. This is perhaps not surprising, as the exclusion of the lower values of [Fe/H] should be expected to have a significant effect on the derived correlations. Interestingly, this result also suggests that previous considerations of this problem, going back to the original claim of Spite & Spite (1982), might have been unduly influenced by the lack of available measurements of $A$(Li) for stars of the lowest metallicity.

When the two predictors are considered in a bivariate regression model, such as model 3, the significance of $A_1$ remains high, while that of $A_2$ increases (at least for the temperature cut $T_{\rm eff} > 5800$ K), reaching marginal (3–4 $\sigma$) significance. The coefficients of determination are also significantly increased in the bivariate regression model, as compared to models 1 and 2. It should be noted that, by excluding the most metal-deficient stars, the collinearity of the predictor variables is markedly decreased.

### REFERENCES


Alonso, A., Arribas, S., & Martínez-Roger, C. 1996, A&AS, 117, 227
Argast, D., Samland, M., Gerhard, O. E., & Thielemann, F.-K. 2000, A&A, 356, 873
Audouze, J., & Silk, J. 1995, ApJ, 451, L49
Beers, T. C., Rossi, S., Norris, J. E., Ryan, S. G., & Shefler, T. 1999, AJ, 117, 981
Beers, T. C., Suzuki, T. K., & Yoshii, Y. 2000, to appear in ASP Conf. Ser., The Light Elements and Their Evolution, ed. L. da Silva, M. Spite, & J. R. Medeiros (San Francisco: ASP), 425
Bell, R. A., & Oke, J. B. 1986, ApJ, 307, 253
Bevington, P. R. 1969, Data Reduction and Error Analysis for the Physical Sciences (New York: McGraw-Hill)
Boesgaard, A. M., Deliyannis, C. P., Stephens, A., & King, J. R. 1998, ApJ, 493, 206
Boesgaard, A. M., King, J. R., Deliyannis, C. P., & Vogt, S. S. 1999, AJ, 117, 492
Boesgaard, A. M., & Tripicco, M. J. 1986, ApJ, 303, 724
Bonifacio, P., & Molaro, P. 1997, MNRAS, 285, 847
Cameron, A. G. W., & Fowler, W. A. 1971, ApJ, 164, 111
Carney, B. W., Latham, D. W., Laird, J. B., & Aguilar, L. A. 1994, AJ, 107, 2240
Cayrel, R., Spite, M., Spite, F., Vangioni-Flam, E., Cassé, M., & Audouze, J. 1999, A&A, 343, 923
Charbonnel, C., & Balachandran, S. 2000, to appear in ASP Conf. Ser., The Light Elements and Their Evolution, ed. L. da Silva, M. Spite, & J. R. Medeiros (San Francisco: ASP), 373
Cottrell, P. L., & Norris, J. 1978, ApJ, 221, 893
Dallal, G. E. 1991, Am. Stat., 45, 74
Deliyannis, C. P., Demarque, P., & Kawaler, S. D. 1990, ApJS, 73, 21
Deliyannis, C. P., Pinsonneault, M. H., & Duncan, D. K. 1993, ApJ, 414, 740
Drake, N. A., de la Reza, R., & da Silva, L. 2000, to appear in ASP Conf. Ser., The Light Elements and Their Evolution, ed. L. da Silva, M. Spite, & J. R. Medeiros (San Francisco: ASP), 502
Fields, B. D., & Olive, K. A. 1999a, ApJ, 516, 797
———. 1999b, NewA, 4, 255
Forestini, M., & Charbonnel, C. 1997, A&A, 123, 241
Fulbright, J. P., & Kraft, R. P. 1999, AJ, 118, 527
Gilroy, K. K., Sneden, C., Pilachowski, C. A., & Cowan, J. J. 1988, ApJ, 327, 298
Gratton, R. 2000, in The Galactic Halo: from Globular Clusters to Field Stars, ed. A Noels & P. Magain, 35th Liège Int. Astroph. Colloq., in press
Gregorio-Hetem, J., Castilho, B. V., Barbuy, B., Spite, F., & Spite, M. 2000, to appear in ASP Conf. Ser., The Light Elements and Their Evolution, ed. L. da Silva, M. Spite, & J. R. Medeiros (San Francisco: ASP), 375
Grevesse, N., & Sauval, A. J. 1998, Space Sci. Rev., 85, 161
Hix, W. R., & Thielemann, K.-F. 1996, ApJ, 460, 869
Hobbs, L. M., & Pilachowski, C. 1988, ApJ, 334, 734
Hobbs, L. M., & Thorburn, J. A. 1994, ApJ, 428, L25
———. 1997, ApJ, 491, 772
Hobbs, L. M., Welty, D. E., & Thorburn, J. A. 1991, ApJ, 373, L47
Hoffman, R. D., Woosley, S. E., Weaver, T. A., Rauscher, T., & Thielemann, F.-K. 1999, ApJ, 521, 735
Israelian, G., García López, R., & Rebolo, R. 1998, ApJ, 507, 805
José, J., & Hernanz, M. 1998, ApJ, 494, 680

King, J. R. 1999, PASP, 111, 817
Kurucz, R. L. 1993, CD-ROM 13, ATLAS 9 Stellar Atmosphere Programs and 2 km/s Grid (Cambridge: SAO)
Lambert, D. L., Heath, J. E., & Edvardsson, B. 1991, MNRAS, 253, 610
Lemoine, M., Vangioni-Flam, E., & Casse, M. 1998, ApJ, 499, 735
Magain, P. 1987, A&A, 181, 323
Matteucci, F., Romano, D., & Molaro, P. 1999, A&A, 341, 458
McWilliam, A., Preston, G., Sneden, C., & Searle, L. 1995, AJ, 109, 2757
Nakamura, T., Umeda, H., Nomoto, K., Thielemann, F.-K., & Burrows, A. 1999, ApJ, 517, 193
Nissen, P. E., Lambert, D. L., Primas, F., & Smith, V. V. 1999, A&A, 348, 211
Norris, J. E., Beers, T. C., & Ryan, S. G. 2000, ApJ, 540, 456
Norris, J. E., Ryan, S. G., Beers, T. C., & Deliyannis, C. P. 1997, ApJ, 485, 370
Norris, J. E., Ryan, S. G., & Stringfellow, G. S. 1994, ApJ, 423, 386
Pagel, B. E. J. 1997, in Nucleosynthesis and Chemical Evolution of Galaxies (Cambridge: Cambridge Univ. Press), chap. 8
Parizot, E., & Drury, L. 1999, A&A, 349, 673
Pinsonneault, M. H., Deliyannis, C. P., & Demarque, P. 1992, ApJS, 78, 179
Pinsonneault, M. H., Walker, T. P., Steigman, G., & Narayanan, V. K. 1999, ApJ, 527, 180
Ramaty, R., Kozlovsky, B., & Lingenfelter, R. E. 1996, ApJ, 456, 525
Rebolo, R., Molaro, P., & Beckman, J. E. 1988, A&A, 192, 192
Romano, D., Matteucci, F., Molaro, P., & Bonifacio, P. 1999, A&A, 352, 117
Rousseeuw, P. J., & Leroy, A. M. 1987, Robust Regression and Outlier Detection (New York: Wiley)
Ryan, S. G. 1989, AJ, 98, 1693
Ryan, S. G., Beers, T. C., Deliyannis, C. P., & Thorburn, J. A. 1996a, ApJ, 458, 543
Ryan, S. G., Beers, T. C., Kajino, T., & Rosolankova, K. 2001, ApJ, 547, 230
Ryan, S. G., Beers, T. C., Olive, K. A., Fields, B. D., & Norris, J. E. 2000, ApJ, 530, L57
Ryan, S. G., & Norris, J. E. 1991, AJ, 101, 1835
Ryan, S. G., Norris, J. E., & Beers, T. C. 1996b, ApJ, 471, 254
———. 1998, ApJ, 506, 892
———. 1999, ApJ, 523, 654
Ryan, S. G., Norris, J. E., & Bessell, M. S. 1991, AJ, 102, 303
Sackmann, I.-J., & Boothroyd, A. I. 1992, ApJ, 392, L71
———. 1999, ApJ, 510, 217
Saxner, M., & Hammarbäck, G. 1985, A&A, 151, 372
Schuster, W. J., & Nissen, P. E. 1988, A&AS, 73, 225
———. 1989, A&A, 222, 65
Schuster, W. J., Parrao, L., & Contreras Martinez, M. E. 1993, A&AS, 97, 951
Smith, V. V., Lambert, D. L., & Nissen, P. E. 1993, ApJ, 408, 262
———. 1998, ApJ, 506, 405
Spite, F., & Spite, M. 1982, A&A, 115, 357
Spite, M., Molaro, P., François, P., & Spite, F. 1993, A&A, 271, L1
Spite, M., Spite, F., Cayrel, R., Hill, V., Depagne, E., Nordstrom, B., & Beers, T. 2000, to appear in ASP Conf. Ser., The Light Elements and Their Evolution, ed. L. da Silva, M. Spite, & J. R. Medeiros (San Francisco: ASP), 356
Steigman, G., & Walker, T. P. 1992, ApJ, 385, L13
Suzuki, T. K., & Yoshii, Y. 2001, ApJ, 548, in press
Suzuki, T. K., Yoshii, Y., & Beers, T. C. 2000, ApJ, 540, 99
Suzuki, T. K., Yoshii, Y., & Kajino, T. 1999, ApJ, 522, L125
Thorburn, J. A. 1992, ApJ, 399, L83
———. 1994, ApJ, 421, 318
Thorburn, J. A., & Beers, T. C. 1992, BAAS, 24, 1278
Timmes, F. X., Woosley, S. E., & Weaver, T. A. 1995, ApJS, 98, 617
Tsujimoto, T., Shigeyama, T., & Yoshii, Y. 1999, ApJ, 519, L63
Vangioni-Flam, E., Cassé, M., Cayrel, R., Audouze, J., Spite, M., & Spite, F. 1999, NewA, 4, 245
Vangioni-Flam, E., Ramaty, R., Olive, K. A., & Casse, M. 1998, A&A, 337, 714
Wilkinson, L., Blank, G., & Gruber, C. 1996, Desktop Data Analysis with Systat (New York: Wiley)
Woosley, S. E., Hartmann, D. H., Hoffman, H. D., & Haxton, W. C. 1990, ApJ, 356, 272
Woosley, S. E., & Weaver, T. A. 1995, ApJS, 101, 181